APPENDIX C

PHOTOCHEMICAL MODELING FOR THE HGB ATTAINMENT DEMONSTRATION SIP REVISION FOR THE 2008 EIGHT-HOUR OZONE STANDARD

APPENDIX C: PHOTOCHEMICAL MODELING FOR THE HGB ATTAINMENT DEMONSTRATION SIP REVISION FOR THE 2008 EIGHT-HOUR OZONE STANDARD

Table of Contents

Appendix C i

Appendix C: Photochemical Modeling for the HGB Attainment Demonstration SIP Revision for the 2008 Eight-Hour Ozone Standard ii

1. Overview 1

2. Performance Comparison with the 2013 HGB 1997 Eight-Hour Ozone MVEB SIP Revision 1

3. Model Performance Snapshots 5

   3.1 Galveston Airport (C1034) 6

   3.2 Conroe Relocated (C78) 7

   3.3 Fayette County (C601) 10

   3.4 Aldine (C8) 12

   3.5 Deer Park (C35) 15

   3.6 Danciger (C618) 19

   3.7 Manvel Croix Park (C84) 20

4. Vertical Ozone Profiles 21

5. Spatiotemporal Distribution of Modeled Ozone Concentrations 23

   5.1 May 16 and 17, 2012 24

   5.2 September 19 through 21, 2012 26

6. Summary 31

1. OVERVIEW

The development of the base case photochemical modeling for this Attainment Demonstration SIP Revision proceeded through a number of iterations, which involved updates and improvements in the meteorological and emissions modeling. The final photochemical modeling configuration is described in Chapter 3. The meteorological modeling is detailed in Appendix A: *Meteorological Modeling for the HGB Attainment Demonstration SIP Revision for the 2008 Eight-Hour Ozone Standard*. Development of the emission inventories is described in Appendix B: *Emissions Modeling for the HGB Attainment Demonstration SIP Revision for the 2008 Eight-Hour Ozone Standard*. Because of the short time for completing this SIP revision, a limited performance evaluation is shown below.

2. PERFORMANCE COMPARISON WITH THE 2013 HGB 1997 EIGHT-HOUR OZONE MVEB SIP REVISION

On January 2, 2014 the EPA approved the 2013 HGB 1997 Eight-Hour Ozone MVEB SIP Revision, which established a motor vehicle emission budget for the area based on the Motor Vehicle Emission Simulator (MOVES). That SIP revision will be referred to as the MOVES SIP. The current modeling has many similarities to the MOVES SIP but significant differences exist beyond updating the emissions and model versions. Most significantly, the current modeling used a single five-month episode in 2012 (May through September), while the MOVES SIP modeling used a 2006 base case which coincided with the TexAQS II field study. The MOVES SIP modeling used three episodes covering June 1 through 15, August 15 through September 14, and September 19 through October 11, 2006, referred to, respectively, as June06, AQS1, and AQS2 (AQS refers to Air Quality Study). The current and MOVES SIP used a Lambert Conformal map Conic projection (LCC), but the current modeling domains cover larger geographic areas in each domain. The current modeling uses the CB6r2h chemical mechanism, which includes halogen chemistry, while the MOVES SIP modeling used the CBo5 chemical mechanism.

In considering the relative performance of the two modeling applications, it is important to remember that the current modeling includes an entire ozone season while the MOVES SIP modeling focused on high-ozone periods. Performance on high-ozone days is important, but since the model is used in a relative sense, model responsiveness is ultimately the key to a modeling demonstration. Since the model's dynamic range may limit its responsiveness, it is important to examine performance during periods of both low and high ozone.

In the following bar charts, statistics calculated for the current SIP revision are displayed in the last five columns in light blue. The MOVES SIP episodes are displayed in the first three columns and are colored light orange.

Horizontal lines represent a compilation of performance statistics from 69 model runs conducted by various organizations during the years 2006 through 2012 (Simon, et al, 2012). These lines allow comparison of the current work to the body of similar analyses conducted in recent years. The solid line represents the median of each statistic presented, and the two lines featuring longer dashes represent the first and third quartiles. The lines with short dashes represent the minimum and maximum values reported across the studies (the minimum value is limited to the first quartile minus 1.5 times the interquartile range, and the maximum is limited to the third quartile plus 1.5 times the interquartile range). A few studies limited the statistical calculations to use only modeled-observed pairs where the observed value exceeded a threshold (usually 40 or 60 ppb), but most used all of the data. The compilations include all studies regardless of whether a threshold was employed.

Figure 2-1: *Mean Bias Comparison, All Modeled-Observed One-Hour Pairs* shows model bias calculated for one-hour average ozone concentrations for the two TCEQ SIP modeling efforts using all modeled-observed data pairs. The bias for the current modeling is much lower than that for the MOVES SIP. Modeling for the first four months of 2012 lies inside the interquartile range of recent studies, with September slightly outside.

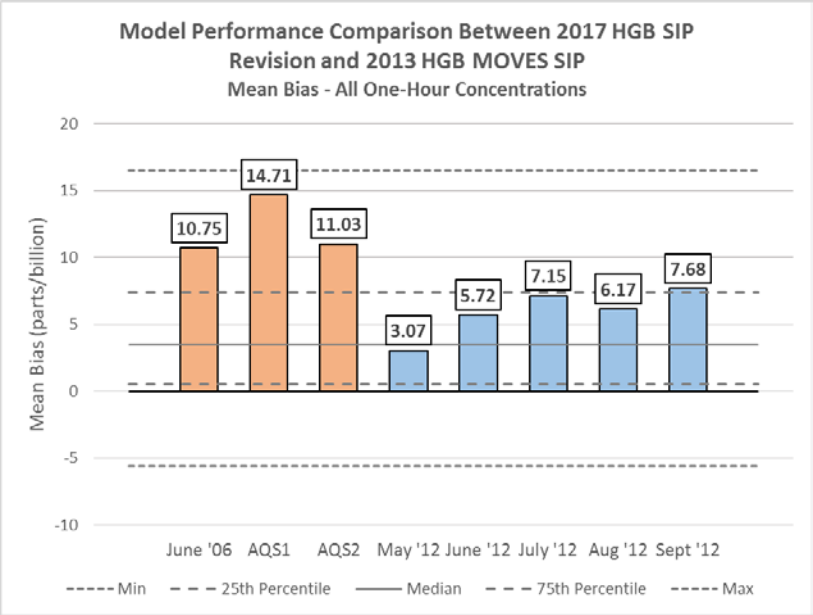

Figure 2-1: Mean Bias Comparison, All Modeled-Observed One-Hour Pairs

While the current modeling shows definite improvement over the MOVES SIP when evaluating over all observed ozone concentrations, the performance differs when values above the 60 ppb threshold are considered. Figure 2-2: *Mean Bias Comparison, Modeled-Observed One-Hour Pairs with Observed Concentration ≥ 60* shows that the model under-predicts higher ozone concentrations in all eight periods considered, although the model has negligible bias in the AQS1 and July 2012 periods. In terms of absolute deviation from zero bias (the goal), both TCEQ modeling configurations fall in the middle of the distribution of compiled model performance statistics.

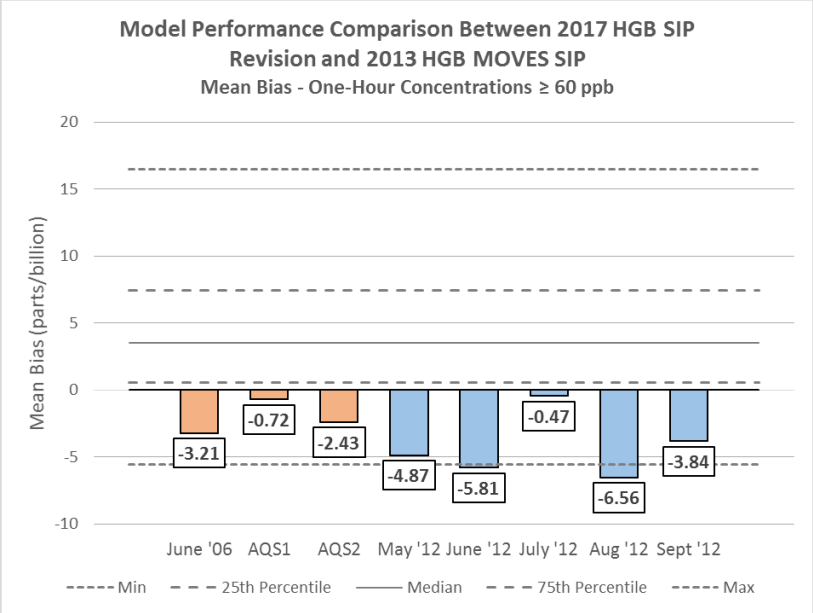

Figure 2-2: Mean Bias Comparison, Modeled-Observed One-Hour Pairs with Observed Concentration ≥ 60 ppb

Figure 2-3: *RMSE Comparison, All Modeled-Observed One-Hour Pairs* shows root mean-square error (RMSE) for the current and MOVES SIP modeling platforms. By this measure, the 2012 modeling performs better than any of the compiled modeling results. The MOVES SIP modeling performed reasonably well, but not as well as the current application.

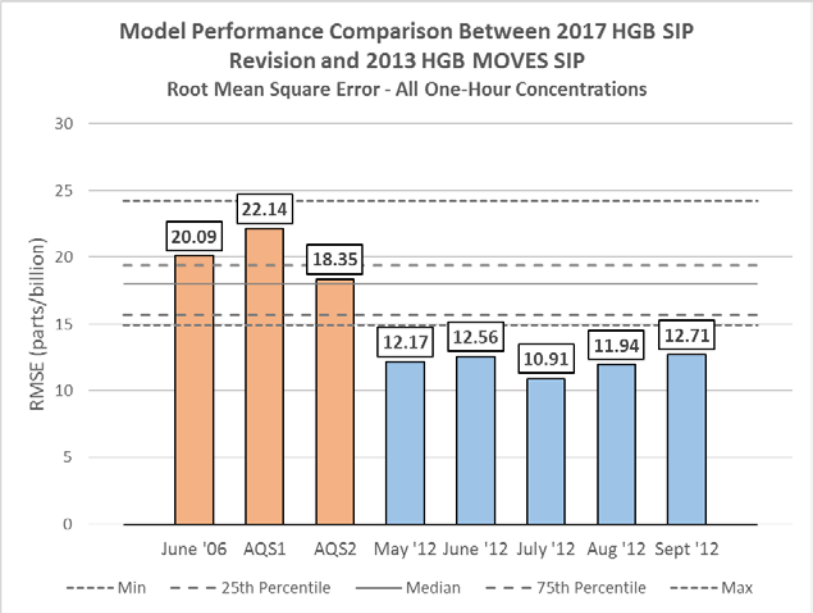

Figure 2-3: RMSE Comparison, All Modeled-Observed One-Hour Pairs

When considering data pairs with observed ozone at or above a 60 ppb threshold, both the current and MOVES SIP modeling compare well with the reference runs, outperforming them

except for the AQS1 and August 2012 periods, as shown in Figure 2-4: *RMSE Comparison, Modeled-Observed One-Hour Pairs with Observed Concentration ≥ 60 ppb*.

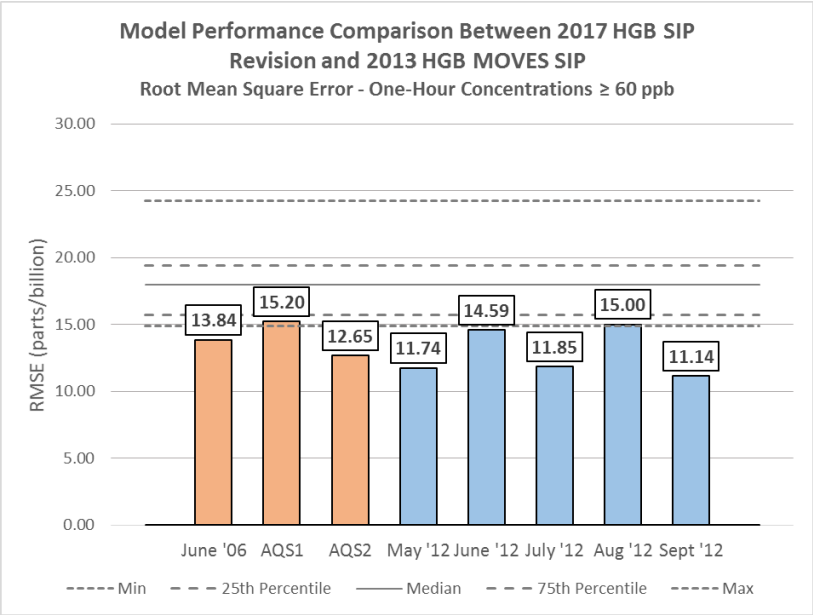

Figure 2-4: RMSE Comparison, Modeled-Observed One-Hour Pairs with Observed Concentration ≥ 60 ppb

For eight-hour ozone concentrations, Figure 2-5: *Mean Bias Comparison, All Modeled-Observed MDA8 Ozone Pairs* compares model bias for maximum daily average eight-hour (MDA8) ozone across the eight modeling periods. When considering all concentration data, model bias is comparable between the MOVES SIP modeling and the 2012 modeling. July shows a significant positive bias, which is expected due to the dominant southerly flow from the Gulf, and some of that bias carries over into August. May, June, and September all have biases below or slightly over the third quartile.

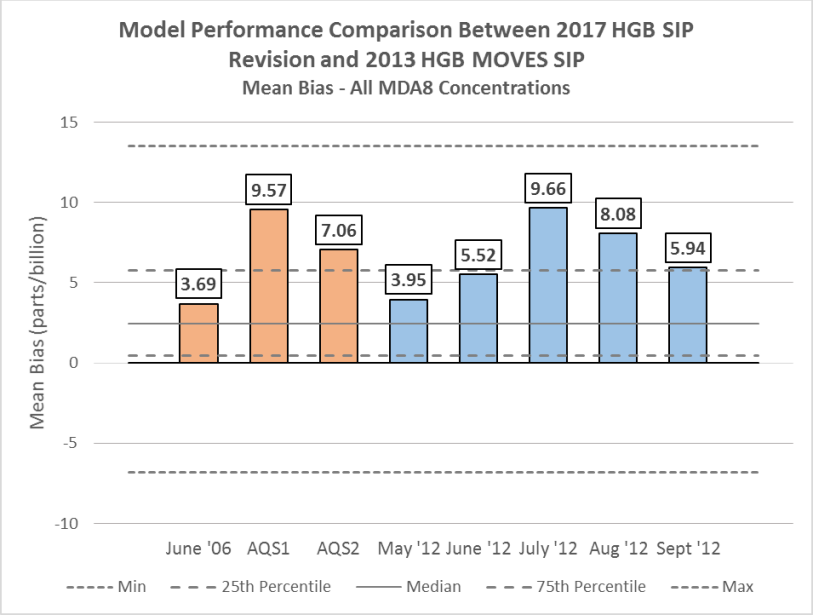

Figure 2-5: Mean Bias Comparison, All Modeled-Observed MDA8 Ozone Pairs

Figure 2-6: *Model Bias for MDA8 Ozone, Data Pairs with Observed Ozone ≥ 60 ppb* shows bias for MDA8 ozone above a threshold of 60 ppb. Only the 2012 modeling is shown since data for the MOVES SIP runs was not available. Also, no data is displayed for July since there were zero days in where any monitor in HGB recorded an MDA8 concentration above 60 ppb.

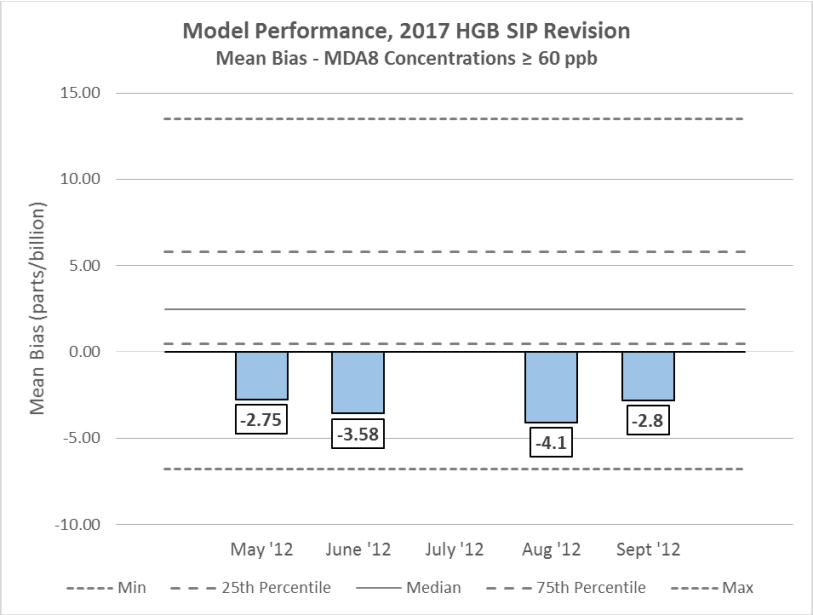

Figure 2-6: Model Bias for MDA8 Ozone, Data Pairs with Observed Ozone ≥ 60 ppb

3. MODEL PERFORMANCE SNAPSHOTS

This section looks at several model performance evaluation methods at selected sites in the HGB nonattainment area to help assess how well CAMx can replicate the physical atmosphere.

3.1 Galveston Airport (C1034)

The first site examined is Galveston Airport - C1034 with its location noted in green in Figure 3-1: *Galveston Airport – C1034 Location*.

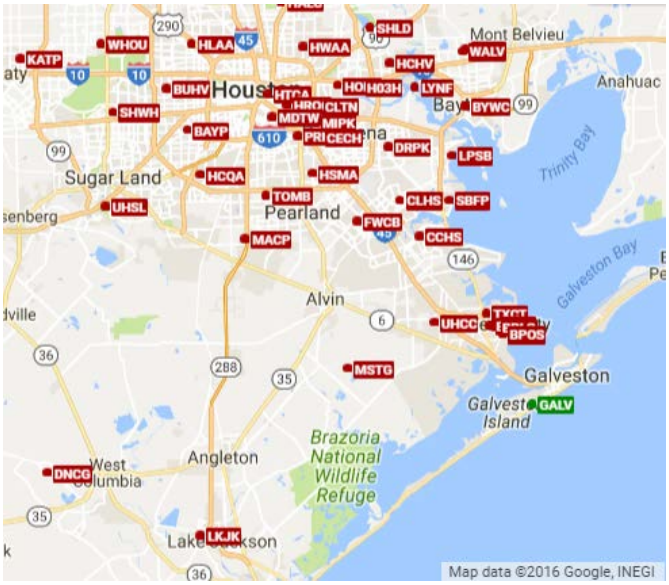

Figure 3-1: Galveston Airport – C1034 Location

Halogen chemistry was first added to CAMx in December 2014 to alleviate the significant over-prediction of ozone concentrations seen along the Texas Coast. The blue line in Figure 3-2: *Time Series of Modeled and Observed Ozone for June 2012 at Galveston Airport – C1034, First Halogen Run vs. No Halogen Chemistry* shows simulated ozone without halogen chemistry, and the green line shows improved performance after halogen chemistry was introduced. While significant over-prediction remained, adding halogen chemistry reduced over-prediction by up to 8 ppb and improved performance for almost the entire month.

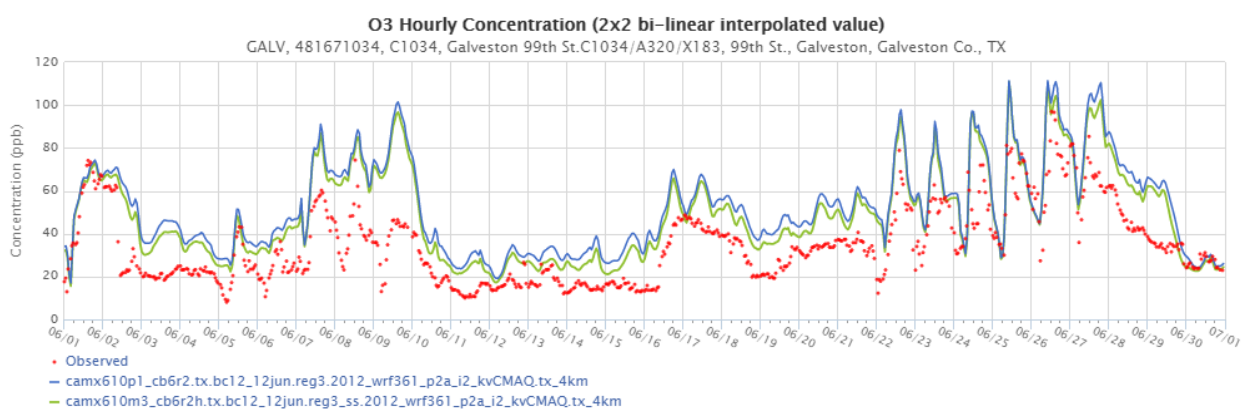

Figure 3-2: Time Series of Modeled and Observed Ozone for June 2012 at Galveston Airport – C1034, First Halogen Run vs. No Halogen Chemistry

Figure 3-2: Time Series of Modeled and Observed Ozone for June 2012 at Galveston Airport – C1034, First Halogen Run vs. No Halogen Chemistry shows a time series comparing the current base case with the first CAMx halogen run (green line in both the figure above and the one below). Additional model refinements over the past 18 months have yielded good model

performance especially on days with higher observed ozone as shown with the blue line for the current model configuration in Figure 3-2.

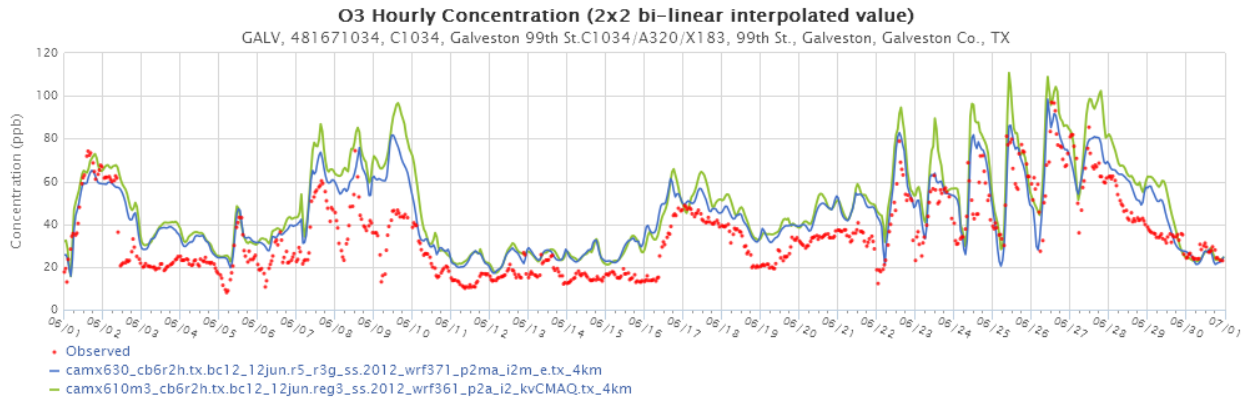

Figure 3-3: Time Series of Modeled and Observed Ozone for June 2012 at Galveston Airport – C1034, Current vs First Halogen Run

3.2 Conroe Relocated (C78)

Conroe C78 is on the opposite (northern) end of the nonattainment area from Galveston (see Figure 3-4: *Conroe Relocated - C78 Location*). Along with significant amounts of local emissions, mostly traffic, Conroe Relocated – C78 is frequently affected by emissions advected northward from the HGB urban core and industries in eastern Harris County. The time series in Figure 3-5: *Time Series of Modeled and Observed Ozone at Conroe – C78 for June 2012* shows good ozone performance for the base case in June 2012 except for over-prediction of the nighttime concentrations during the last half of the episode. Figure 3-6: *Time Series of Modeled and Observed Ozone at Conroe – C78 for August 2012* shows the same figure for August where model performance again is good, except for over-predicting some peak daily concentrations in the 60-75 ppb range. In Figure 3-7: *Time Series of Modeled and Observed Ozone at Conroe – C78 for September 2012*, model performance on the peaks is exemplary, although again some of the lower nighttime values are over-predicted. Time series plots showing a single model run include bands showing the minimum and maximum concentrations within the 3x3 grid cell array containing the monitor.

Figure 3-4: Conroe Relocated - C78 Location

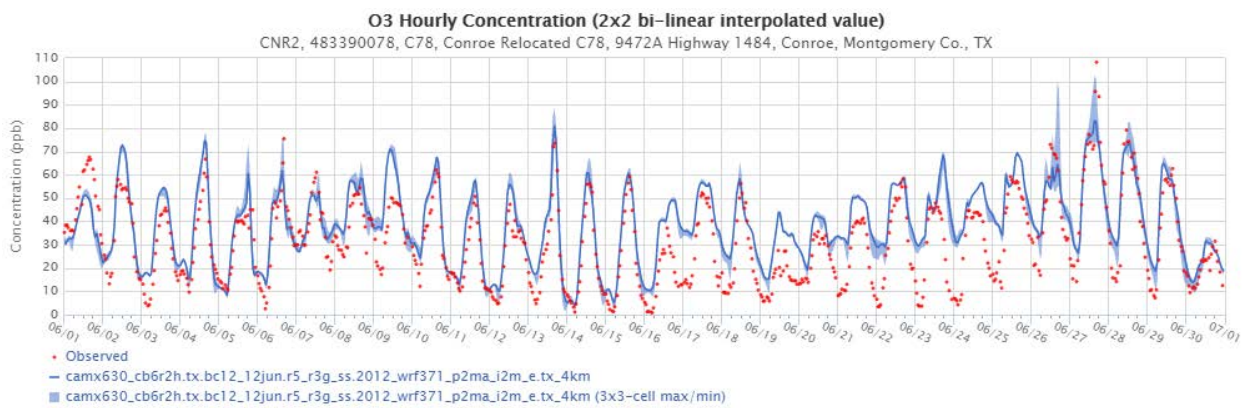

Figure 3-5: Time Series of Modeled and Observed Ozone at Conroe – C78 for June 2012

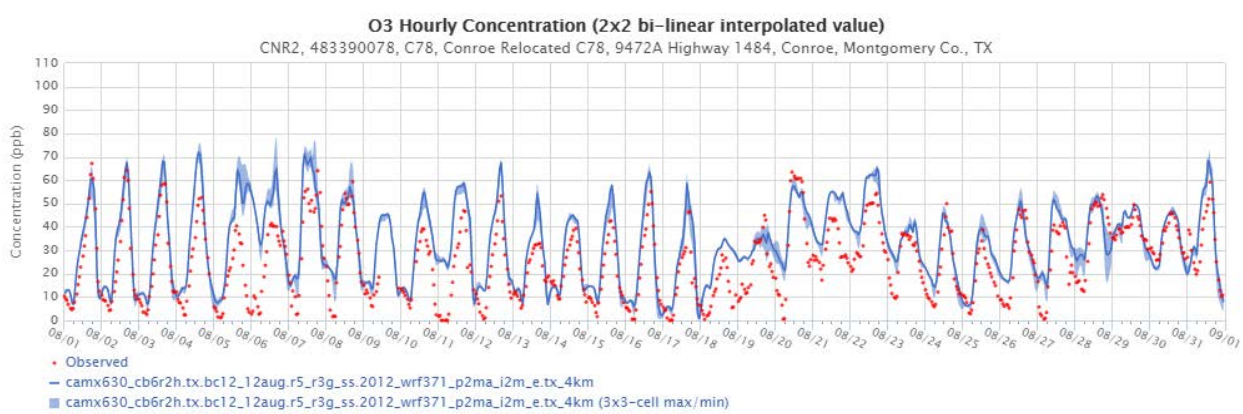

Figure 3-6: Time Series of Modeled and Observed Ozone at Conroe – C78 for August 2012

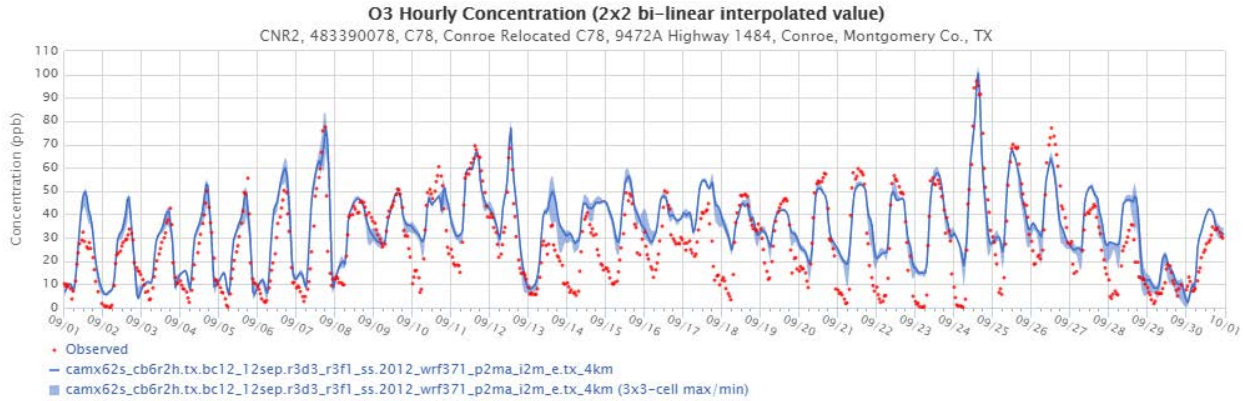

Figure 3-7: Time Series of Modeled and Observed Ozone at Conroe – C78 for September 2012

Figure 3-8: *Time series of Modeled and Observed NO_X at Conroe – C78 for June 2012* shows the June time series for NO_X at Conroe Relocated, and offers some explanation for the model nighttime ozone over-prediction. The model over-estimates NO_X concentrations between 21:00 and 06:00, which implies ozone is being titrated. Inadequate mixing in the first couple of hundred meters is a suspected cause. Meanwhile daytime NO_X appears to be under-estimated. The wide blue bands show that modeled NO_X varies widely among grid cells, reinforcing the notion of incommensurability between a point measurement and the volume of a 4x4 km grid cell in which it is located. Performance can be affected by a monitor's location within a grid cell.

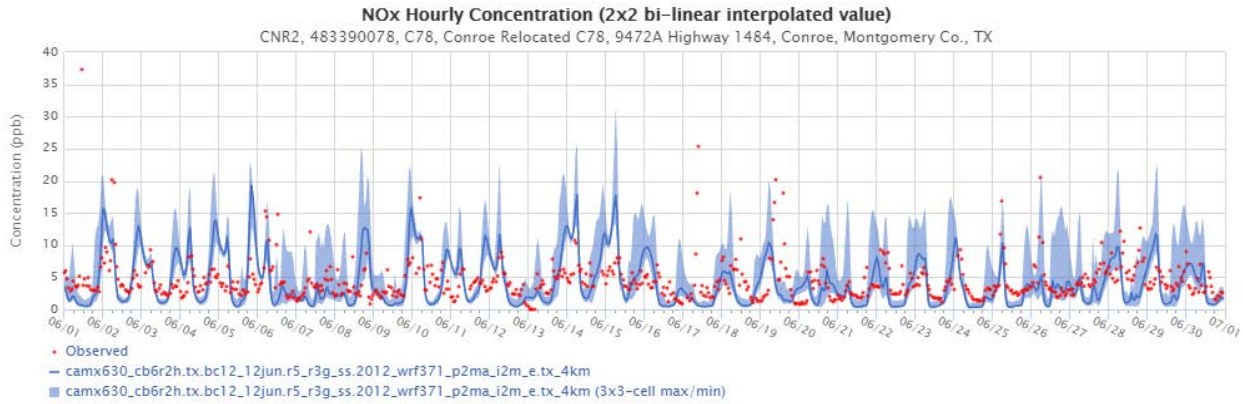

Figure 3-8: Time series of Modeled and Observed NO_X at Conroe – C78 for June 2012

Figure 3-9: *Cumulative Density Plot of Modeled and Observed NO_X at Conroe – C78 for June 2012* presents another view of the NO_X concentrations. This plot compares the modeled and observed cumulative densities. Although the observations in this plot are unpaired in space and time, it shows how well the model represents the distribution of observed concentrations. The vertical gradients represent deciles of the respective distributions: first decile (0.1) shows 10% of the observed values lie below about 2 ppb, while 10% of modeled concentrations lie below 0.6 ppb. At the median (0.5) half of the observations are below 3.7 ppb, while half of the modeled concentrations are below 2.7 ppb. About two-thirds of both observed and modeled distributions lie below 4.7 ppb. Beyond this point, the modeled distribution overtakes the observations until approximately the 98th percentile, where some extreme observations push the observed

distribution ahead. In short, the model has fewer low (< 4.6 ppb) concentrations than observed, but has more above 4.6 ppb except for a few extreme observations.

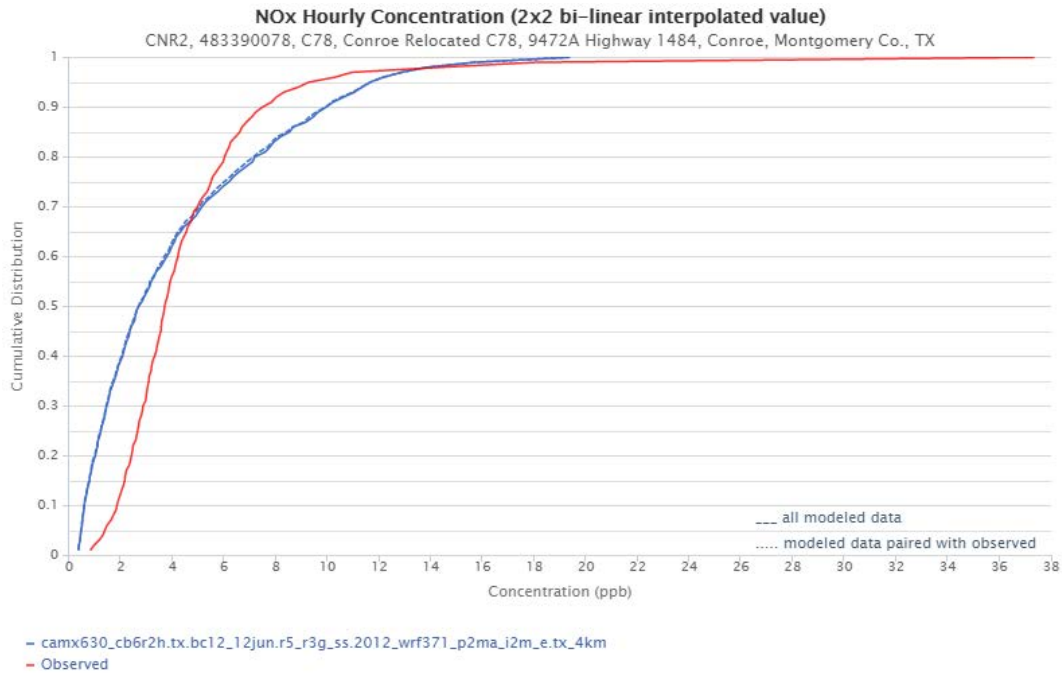

Figure 3-9: Cumulative Density Plot of Modeled and Observed NO_X at Conroe – C78 for June 2012

3.3 Fayette County (C601)

Fayette County - C601 is a rural site located northwest of the HGB nonattainment area, as shown in Figure 3-10: *Fayette County – C601 Location*. Although Fayette County is not normally a background site for HGB, it is occasionally a downwind site and is representative of the model's ability to replicate ozone concentrations in an area with urban influence. Figure 3-11: *Time Series of Modeled and Observed Ozone at Fayette County – C601 for June 2012*, Figure 3-12: *Time Series of Modeled and Observed Ozone at Fayette County – C601 for July 2012*, and Figure 3-13: *Time Series of Modeled and Observed Ozone at Fayette County for August 2012* show time series for June through August, respectively, at Fayette County – C601. Throughout the period shown the model does a very credible job of following the rise and fall of ozone and matching the peaks, although there is a tendency to over-predict very low concentrations in the early morning. These low observed concentrations most likely result from ozone titration caused by fresh NO_X emissions near the monitor being trapped beneath a nocturnal inversion and may result from localized effects beyond the 16 km^2 resolution of the model. In July, observed concentrations are low throughout the month, a trend reflected well in

the model. August performance is reasonable. The model missed the observed peak on August 20, a day that saw widespread high ozone over much of the southern half of Texas.

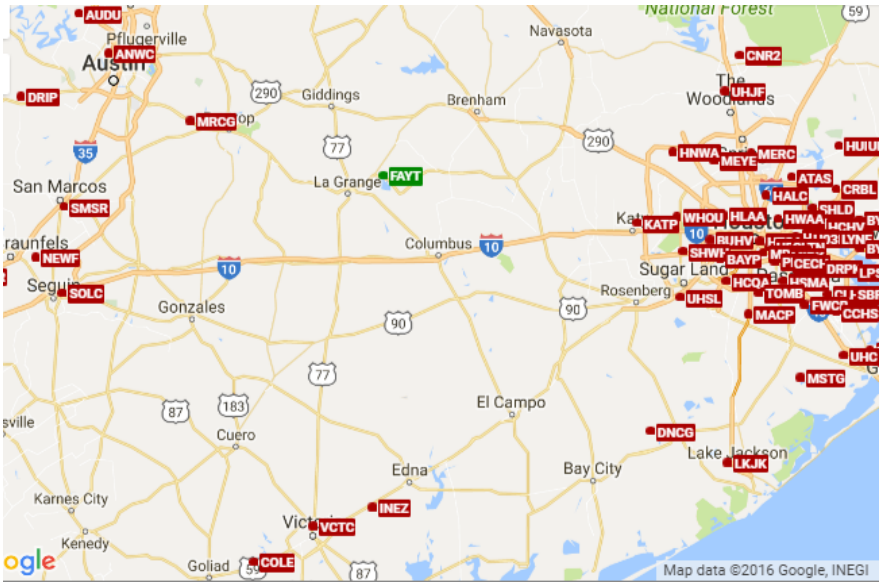

Figure 3-10: Fayette County – C601 Location

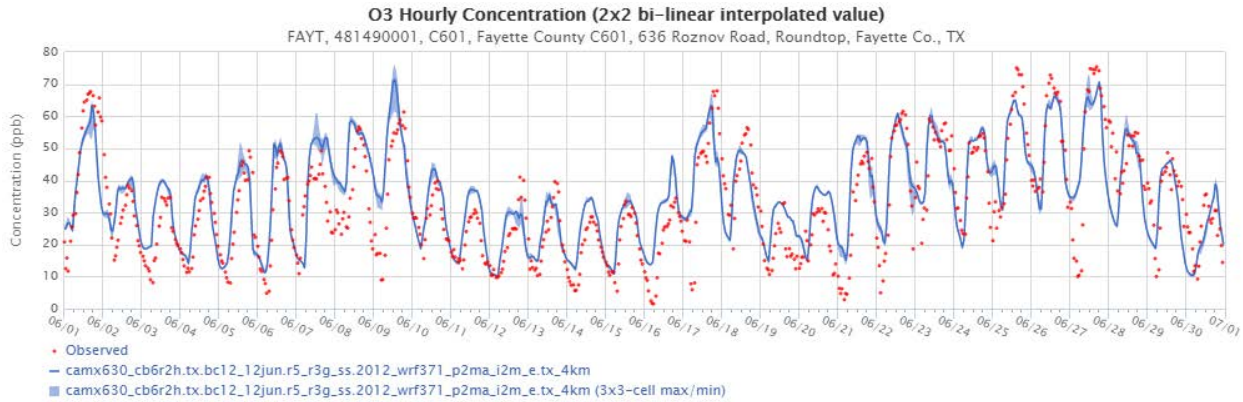

Figure 3-11: Time Series of Modeled and Observed Ozone at Fayette County – C601 for June 2012

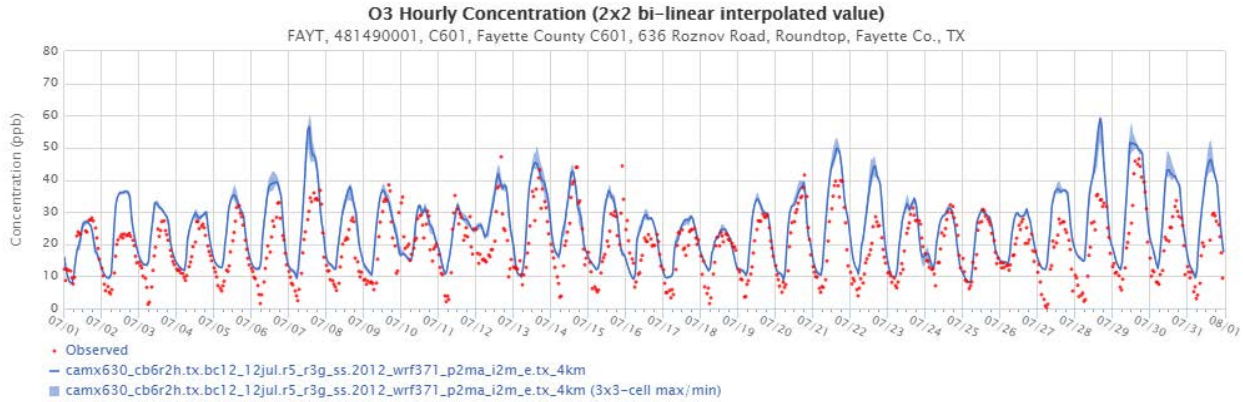

Figure 3-12: Time Series of Modeled and Observed Ozone at Fayette County – C601 for July 2012

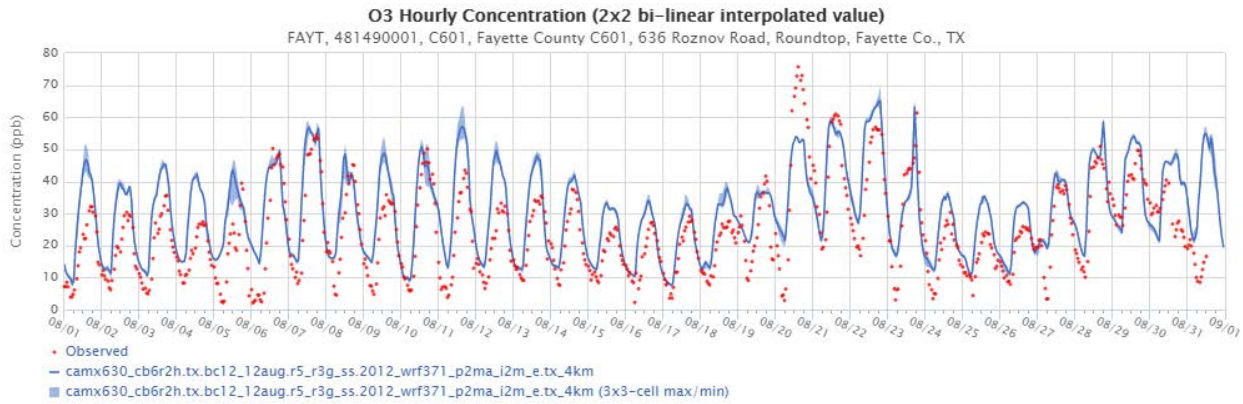

Figure 3-13: Time Series of Modeled and Observed Ozone at Fayette County for August 2012

3.4 Aldine (C8)

Aldine – C8 is a suburban site that is occasionally downwind of the Houston Ship Channel or the Houston urban core (see Figure 3-14: *Aldine – C8* Location). Figure 3-15: *Time Series of Modeled and Observed Ozone at Aldine – C8 for June 2012*, Figure 3-16: *Time Series of Modeled and Observed NO_X at Aldine – C8 for June 2012*, and Figure 3-17: *Time Series of Modeled and Observed CO at Aldine – C8 for June 2012* show time series of observed and modeled ozone, NO_X, and CO, respectively for Aldine – C8 for June 2012. Ozone performance is generally good, replicating the high peaks observed on June 26 and 27 well. Performance of NO_X and CO is also good, especially considering the localized nature of roadways and other NO_X and CO sources compared with the 4 km grid cell size.

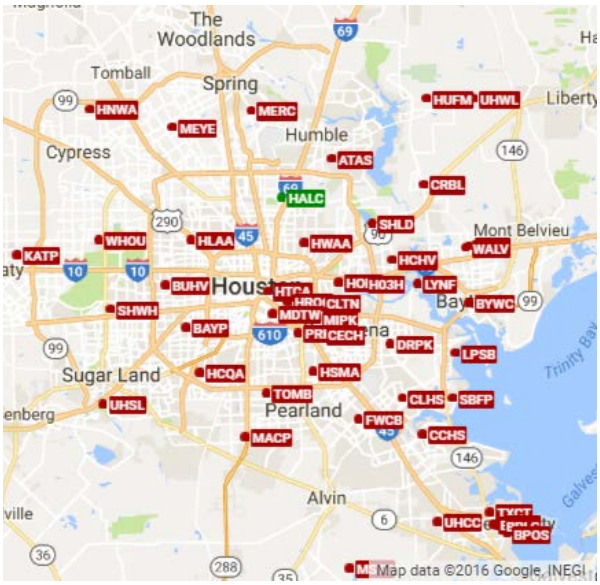

Figure 3-14: Aldine – C8 Location

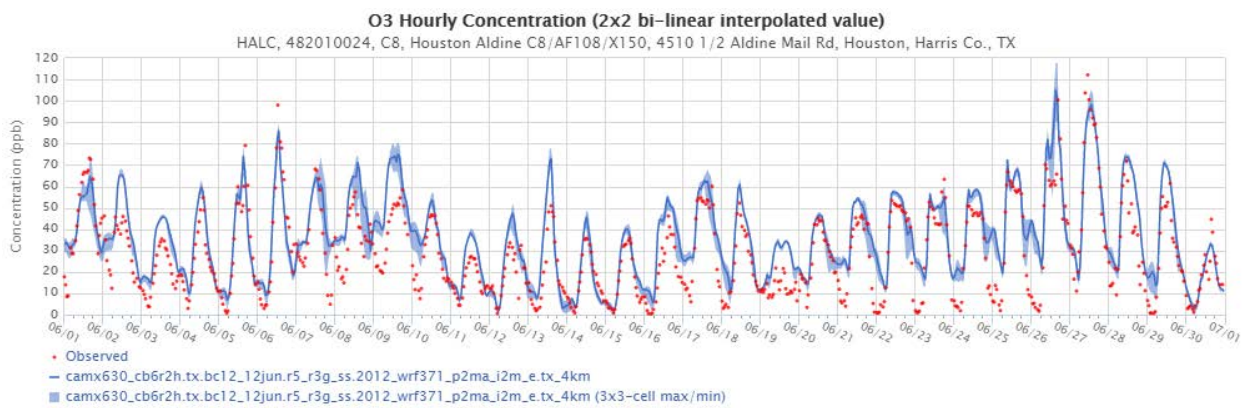

Figure 3-15: Time Series of Modeled and Observed Ozone at Aldine – C8 for June 2012

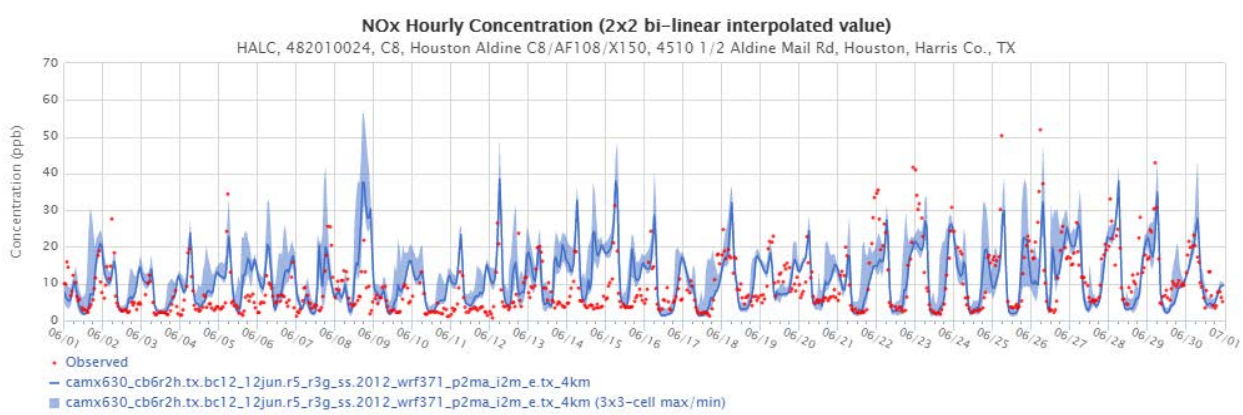

Figure 3-16: Time Series of Modeled and Observed NO_X at Aldine – C8 for June 2012

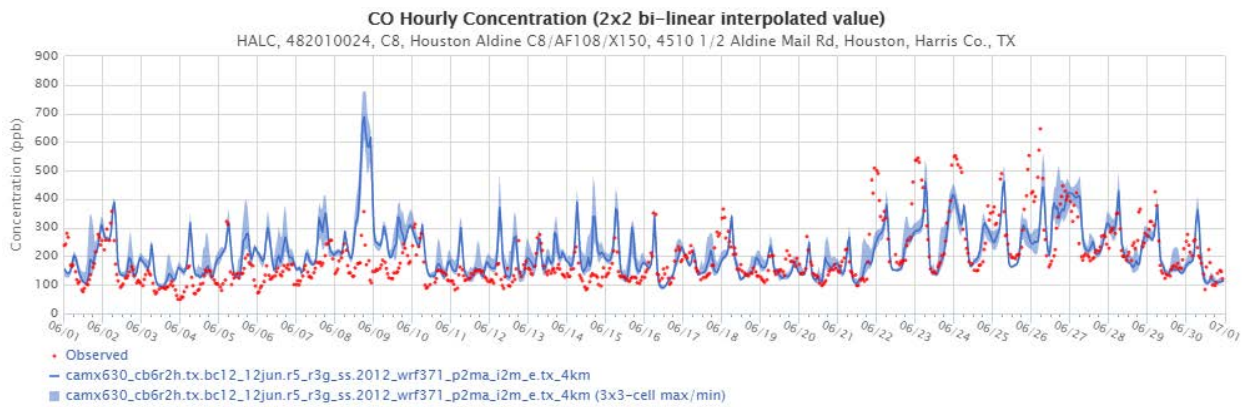

Figure 3-17: Time Series of Modeled and Observed CO at Aldine – C8 for June 2012

Figure 3-18: *Cumulative Density Plot of Modeled and Observed NO_X at Aldine – C8 for June 2012* and Figure 3-19: *Cumulative Density Plot of Modeled and Observed CO at Aldine – C8 for June 2012* show cumulative density plots of the NO_X and CO data displayed above, and show a modest positive bias for both pollutants. Median modeled NO_X concentration is 10.05 ppb compared with observed median of 6.27 ppb, while modeled median CO concentration is 188.23 ppb compared with an observed median of 158.9 ppb.

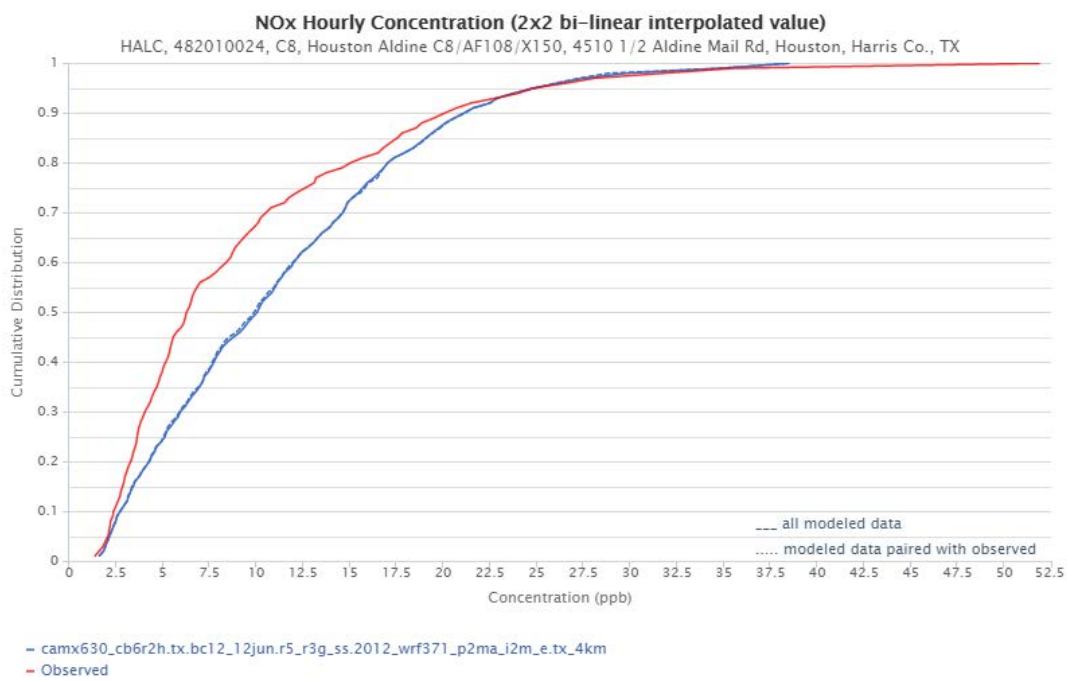

Figure 3-18: Cumulative Density Plot of Modeled and Observed NO_X at Aldine – C8 for June 2012

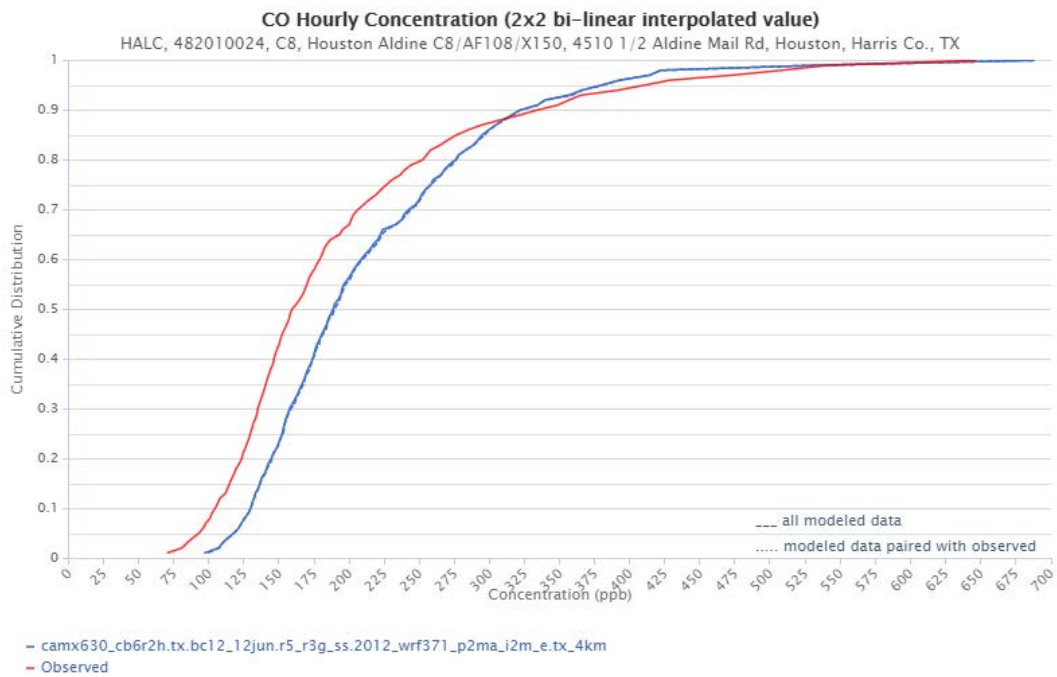

Figure 3-19: Cumulative Density Plot of Modeled and Observed CO at Aldine – C8 for June 2012

3.5 Deer Park (C35)

Deer Park - C35 is located south of the Ship Channel industrial area (Figure 3-20: *Deer Park – C35* Location). This site measures not only ozone, NO_X, and CO but also collects hourly speciated hydrocarbon data using an automated gas chromatograph (auto-GC). Figure 3-21: *Time Series of Modeled and Observed Ozone at Deer Park – C35 for August 2012* shows observed and modeled ozone concentrations for August 2012. The model matches the peak concentrations well temporally, but under-predicts all three peaks above 90 ppb by 10 to 15 ppb. The model over-predicts some peaks in the 40 ppb range, but does well matching the early morning lows. Figure 3-22: *Time Series of Modeled and Observed NO_X at Deer Park – C35 for August 2012* shows a tendency to over-predict NO_X, although the model predicts morning peak concentrations reasonably well. Figure 3-23: *Time Series of Modeled and Observed CO at Deer Park – C35 for August 2012* compares modeled and observed CO, and shows a relatively strong tendency to over-predict CO concentrations outside the August 20 through 27 period.

Figure 3-20: Deer Park – C35 Location

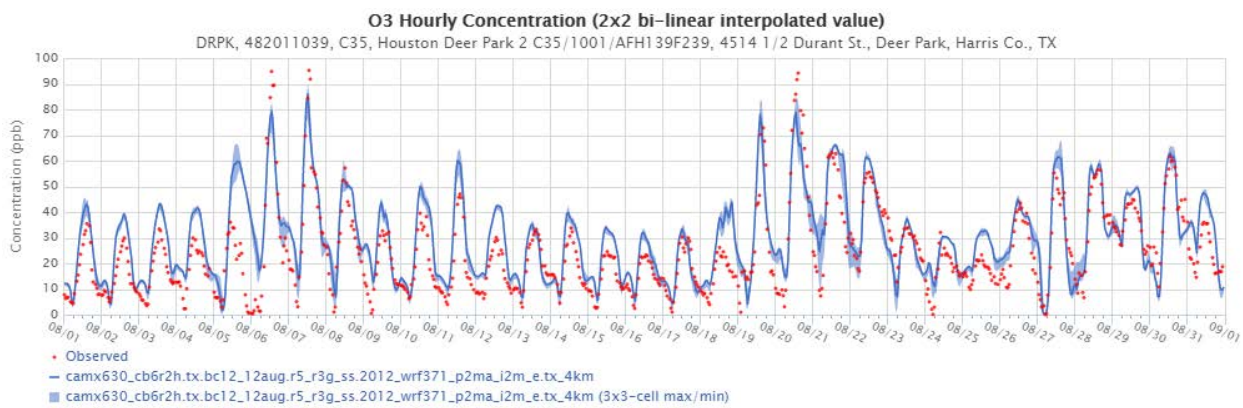

Figure 3-21: Time Series of Modeled and Observed Ozone at Deer Park – C35 for August 2012

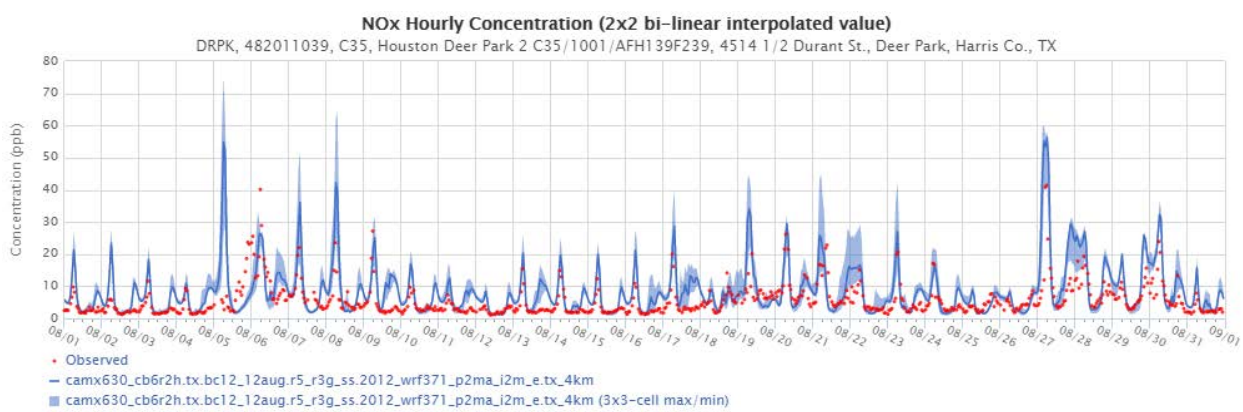

Figure 3-22: Time Series of Modeled and Observed NO_X at Deer Park – C35 for August 2012

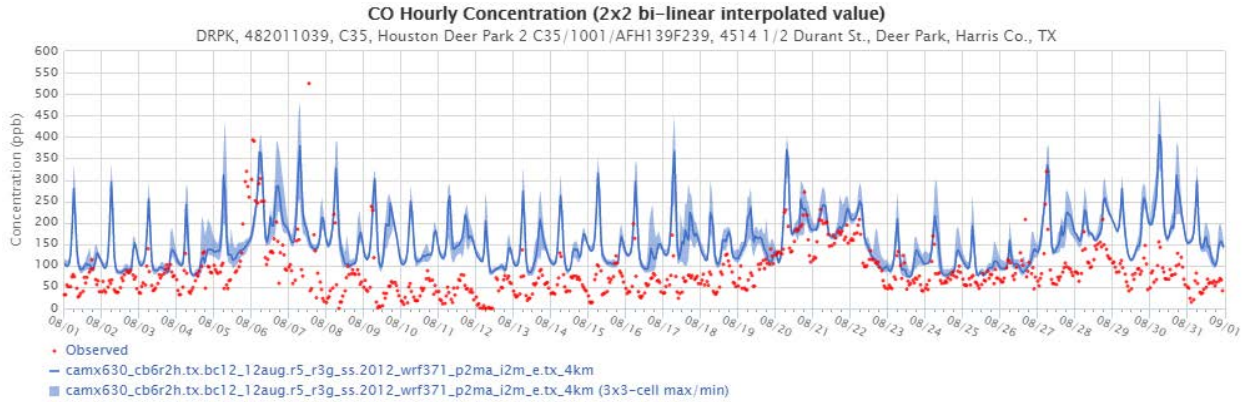

Figure 3-23: Time Series of Modeled and Observed CO at Deer Park – C35 for August 2012

The next several figures show time series comparing several CB6 hydrocarbon species with observations. With a few exceptions (most notably ETH – ethene, ETHA – ethane, PRPA – propane, and ISOP – isoprene) the actual hydrocarbon data undergo a transformation according to the carbon-carbon bond structure for comparison to photochemical model output. For example, PAR represents a single C-C bond, which is found in a large variety of organic molecules, so the CB6 PAR species represents all or part of many different atmospheric chemicals. Figure 3-24: *Time Series of Modeled and Observed ETH (ethene) at Deer Park – C35 for August 2012* and Figure 3-25: *Time Series of Modeled and Observed OLE (certain olefins) at Deer Park – C35 for August 2012* show that ETH and OLE, two highly-reactive CB6 species, tend to be over-predicted overnight. On the other hand, daytime concentrations are modeled fairly well on most days, as shown in Figure 3-26: *Time Series with Reduced Scale of Modeled and Observed OLE (certain olefins) at Deer Park – C35 for August 2012*.

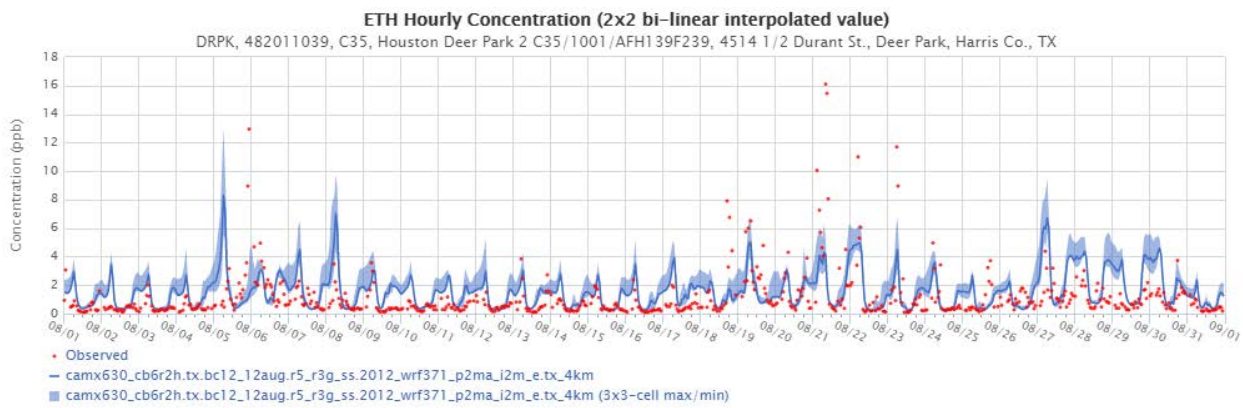

Figure 3-24: Time Series of Modeled and Observed ETH (ethene) at Deer Park – C35 for August 2012

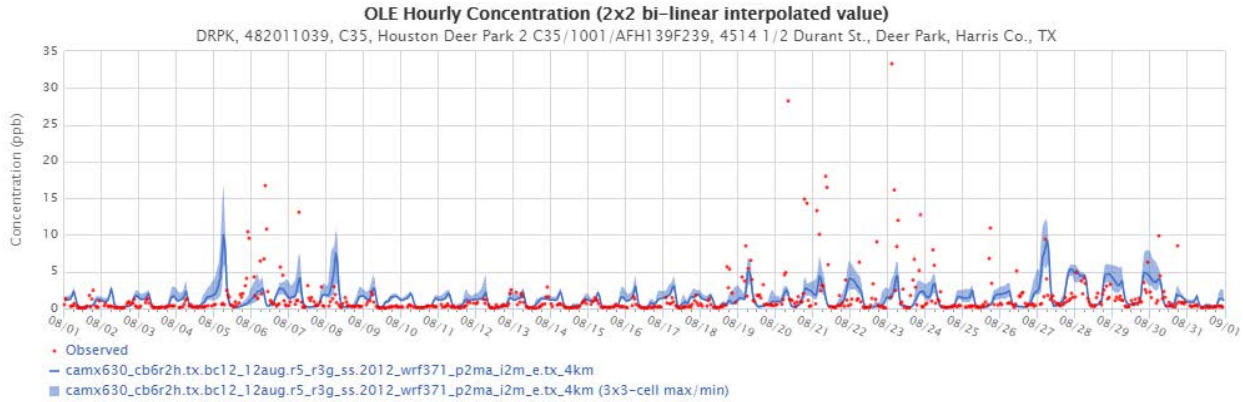

Figure 3-25: Time Series of Modeled and Observed OLE (certain olefins) at Deer Park – C35 for August 2012

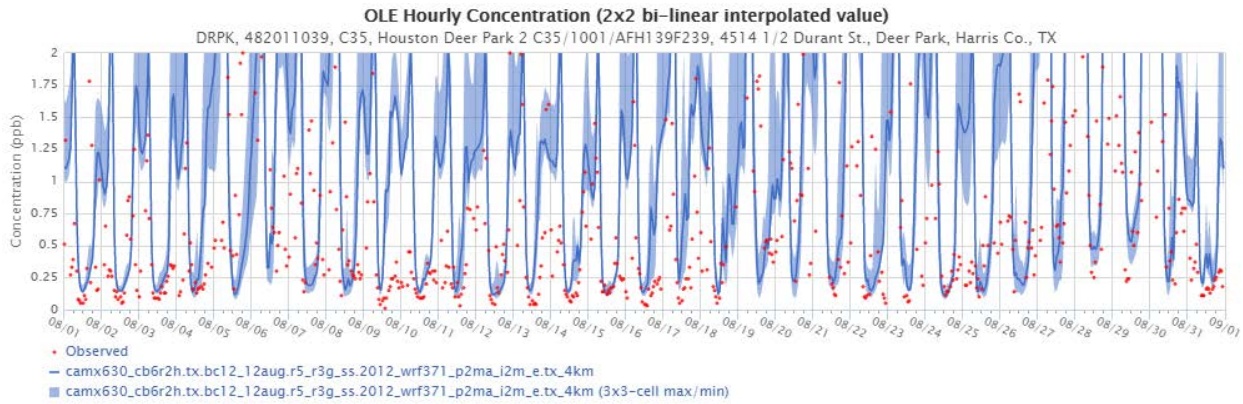

Figure 3-26: Time Series with Reduced Scale of Modeled and Observed OLE (certain olefins) at Deer Park – C35 for August 2012

Figure 3-27: *Time Series of Modeled and Observed PAR at Deer Park – C35 for August 2012* shows the time series for the CB6 species PAR. On many nights the observed concentrations were relatively low, under 30 ppb, and in these cases the model usually over-predicted the concentrations. However, during periods when the overnight/early morning concentrations were higher, specifically August 3 through 9, August 19 through 24, and August 27 through 30 the model also produced higher concentrations and matched the timing of the observed concentration increases and decreases well.

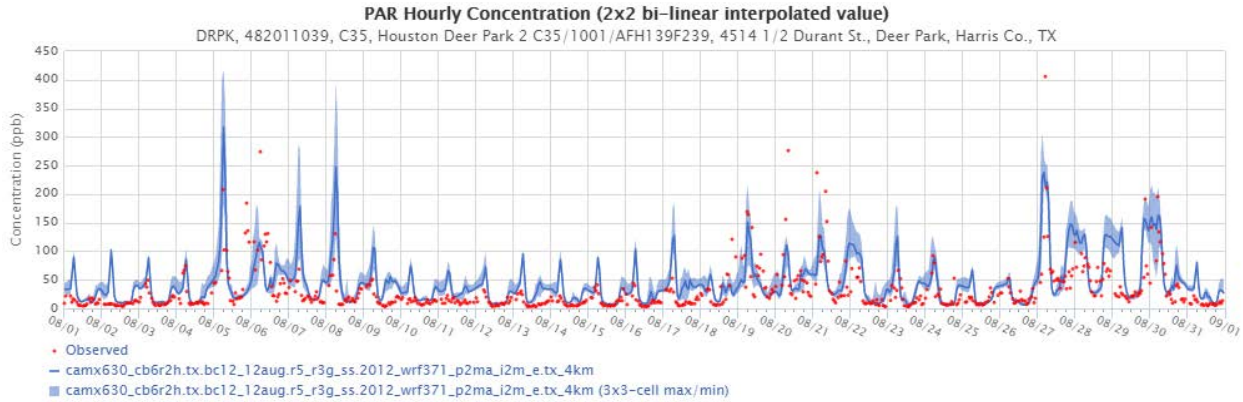

Figure 3-27: Time Series of Modeled and Observed PAR at Deer Park – C35 for August 2012

3.6 Danciger (C618)

Danciger – C618 is an auto-GC site and its rural location makes it a good site for evaluating biogenic isoprene concentrations in the model (Figure 3-28: *Danciger – C618 Location*). Figure 3-29: *Time Series of Modeled and Observed ISOP (isoprene) at Danciger – C618 for September 2012* shows a time series of modeled and observed isoprene concentrations for September 2012 and shows that the model matches the diurnal variation very well, although the model sometimes misses the highest concentrations. A large petrochemical facility a few miles south of the monitor may add to the observed isoprene concentrations under certain conditions.

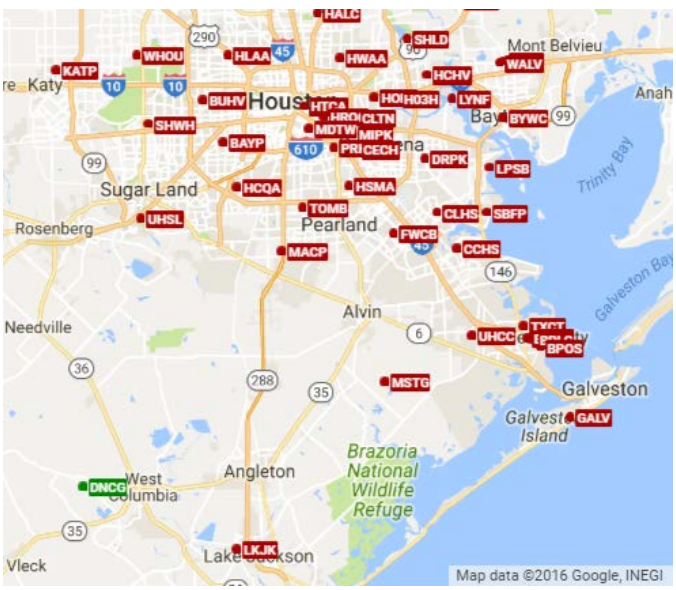

Figure 3-28: Danciger – C618 Location

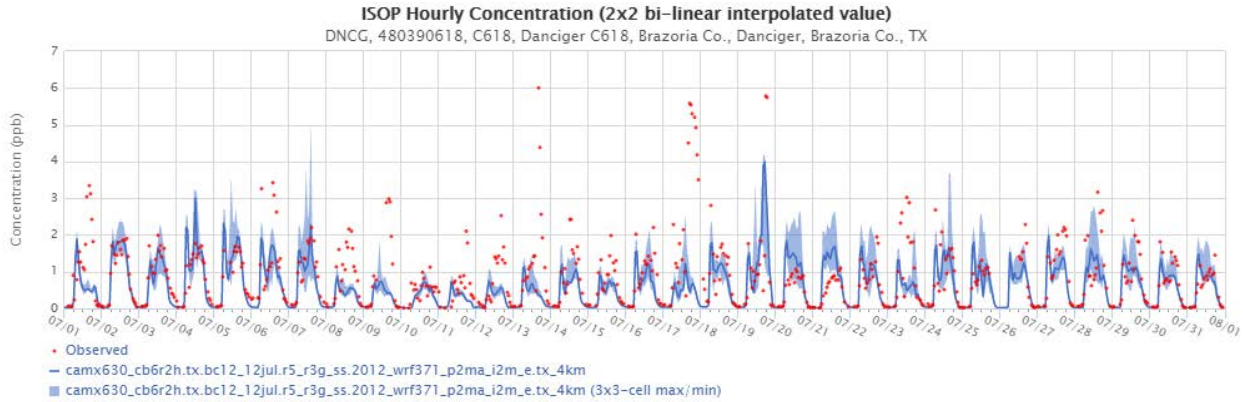

Figure 3-29: Time Series of Modeled and Observed ISOP (isoprene) at Danciger – C618 for September 2012

3.7 Manvel Croix Park (C84)

Manvel Croix Park - C84 (Figure 3-30: *Manvel Croix Park – C84 Location*) has frequently recorded some of the highest MDA8 ozone concentrations in the HGB area in recent years. Figure 3-31: *Time Series of Modeled and Observed Ozone at Manvel Croix Park – C84 for August 2012* shows a time series of modeled and observed ozone concentrations for August 2012. For the first 18 days the model does a good job replicating low to moderate peaks, but tends to over-predict the very low early morning concentrations. Beginning on August 19 through 23 the overnight concentrations are much higher and the model replicates them fairly well. On August 20 and 21 the monitor recorded the highest one-hour concentrations of the month and the model replicates the timing of those peaks well but falls short of matching the amplitude. The model does a better job of matching the peak on August 27 and again matches the timing of the peak on August 28 but not the magnitude. During the two late-month periods of elevated ozone the model matches the lower ozone concentrations fairly well.

Figure 3-30: Manvel Croix Park – C84 Location

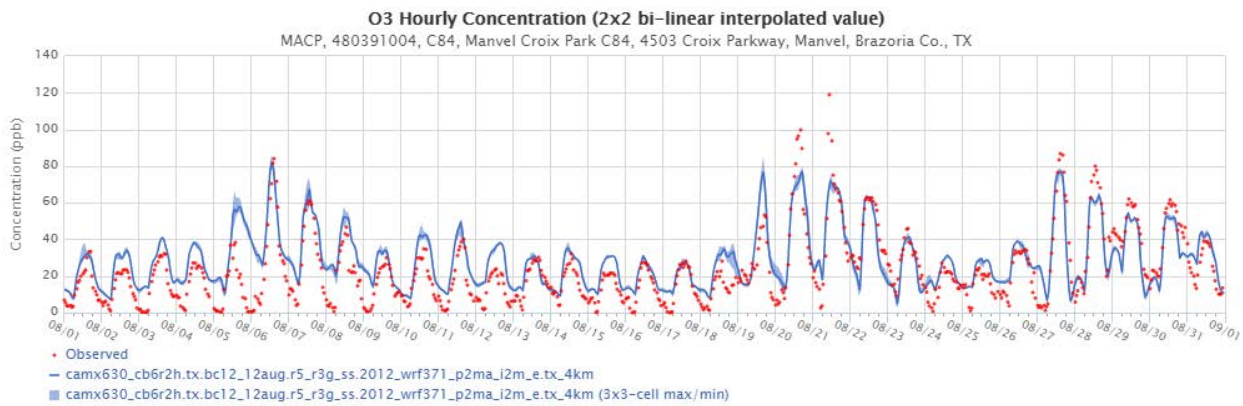

Figure 3-31: Time Series of Modeled and Observed Ozone at Manvel Croix Park – C84 for August 2012

Figure 3-32: *Cumulative Density Plot of Modeled and Observed NO_X at Manvel Croix Park – C84 for August 2012* shows a CDF plot of modeled and observed NO_X at Manvel for the month of August, and shows generally low observed concentrations. Over most of the distribution of observed NO_X the model shows a fairly constant bias of around 1.5 ppb.

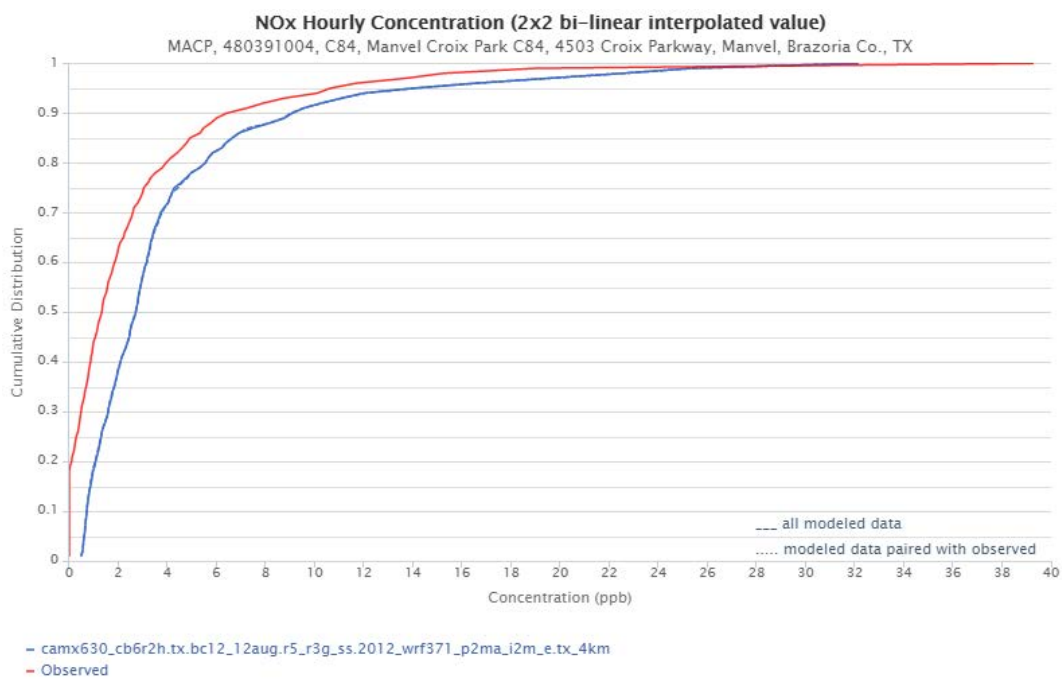

Figure 3-32: Cumulative Density Plot of Modeled and Observed NO_X at Manvel Croix Park – C84 for August 2012

4. VERTICAL OZONE PROFILES

During the period May through September 2012 there were a total of 20 ozone sonde launches in the Houston area, most from the University of Houston campus near downtown Houston. Figure 4-1: *June 2012 Ozone Sonde Launches in the Houston Area* compares observed and

modeled ozone concentrations for the four launches in June 2012. On the first three launches the observed concentrations are fairly constant with increasing altitude to the top of the mixed layer, where they decrease rapidly in the course of a couple of hundred meters. On June 1 and 6 the model shows the same behavior except that modeled concentrations are lower than observed. On June 26, the day that recorded the highest MDA8 ozone concentration of 2012, the model did not show a clear discontinuity at the top of the mixed layer and modeled concentrations at the surface were much lower than observed at the launch site. On the following day's 10:00 launch, neither the model nor the balloon saw a distinct boundary layer and modeled and observed ozone concentrations did not diverge widely until around 10 km above the ground.

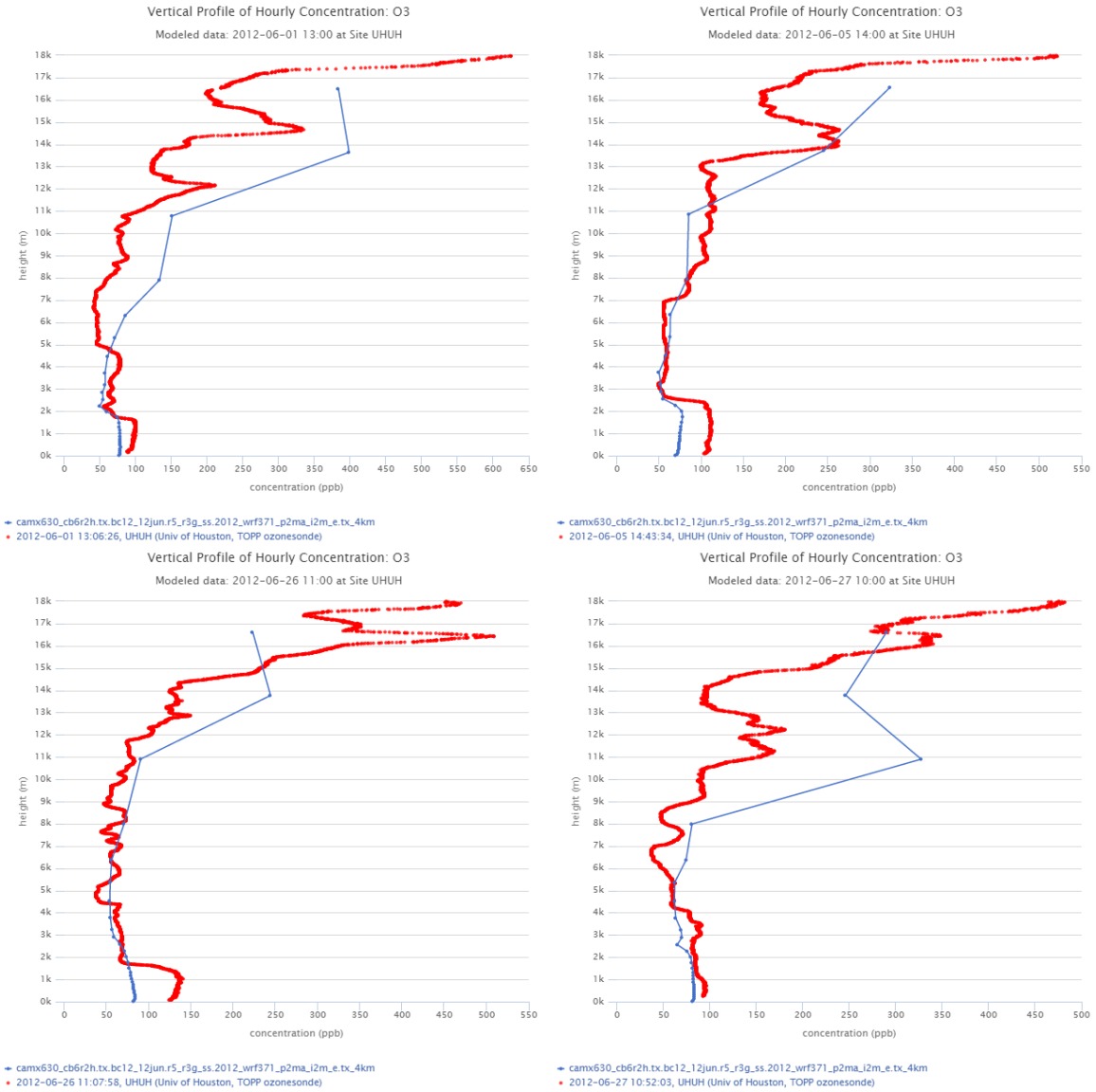

Figure 4-1: June 2012 Ozone Sonde Launches in the Houston Area

Figure 4-2: *September 2012 Ozone Sonde Launches in the Houston Area* compares observed and modeled ozone for the four September sonde launches. The observed ozone concentrations indicated a boundary layer at 2 km on September 8, which was not replicated by the model. On September 21 the ozone sonde indicated a boundary layer at approximately 1.8 km, which was evident in the model. For all four days the model tracked observed ozone concentrations very

well to above 10 km, where modeled upper tropospheric concentrations exceeded the observations.

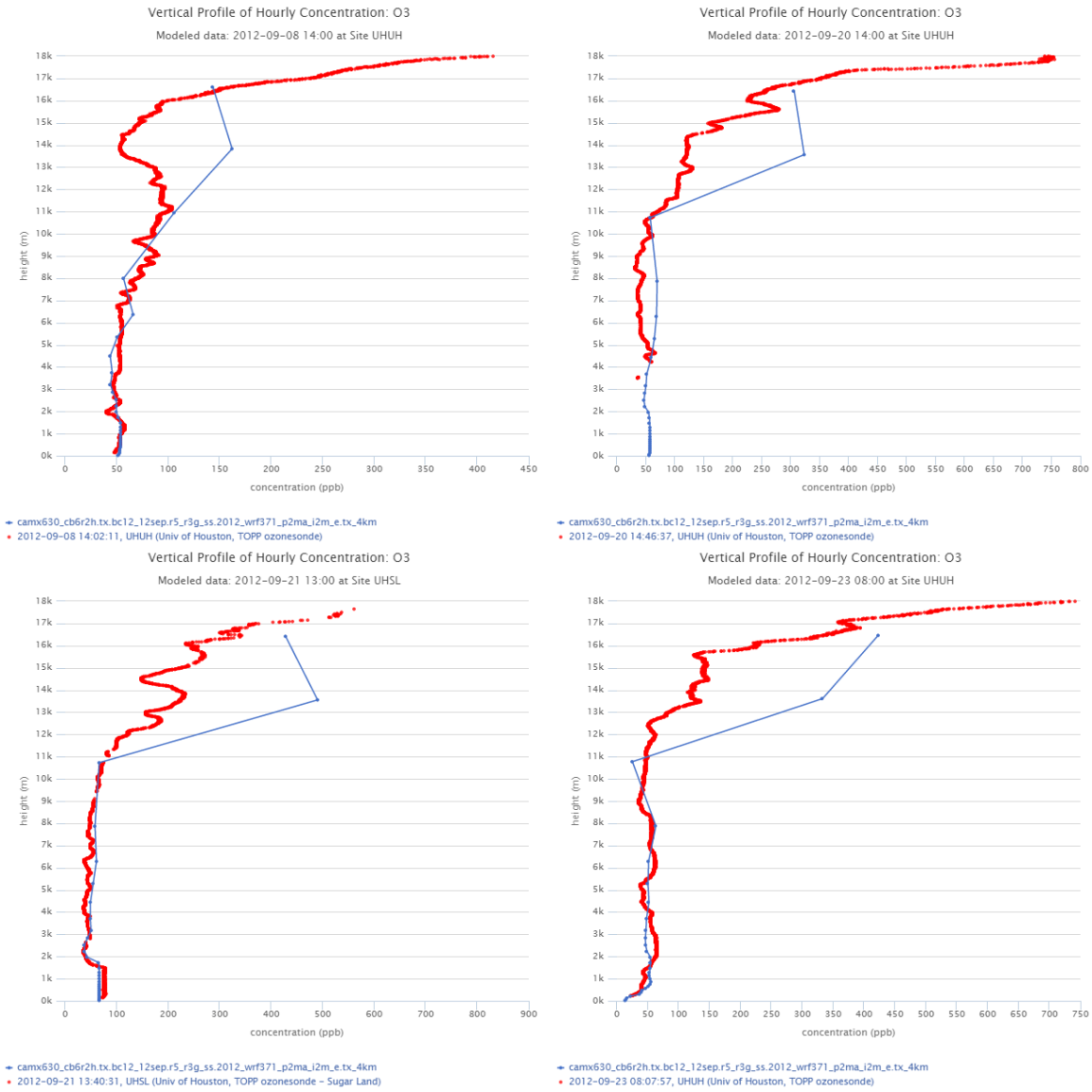

Figure 4-2: September 2012 Ozone Sonde Launches in the Houston Area

5. SPATIOTEMPORAL DISTRIBUTION OF MODELED OZONE CONCENTRATIONS

This section examines the ability of the model to put high ozone concentrations in the right place. Because it is not possible to exactly replicate wind speed and direction, vertical mixing, cloud cover, and chemical processing in any model, the raw output concentrations will never exactly replicate the observations. Visual inspection of output fields provides a good approach to evaluating how close the model comes.

The plots in this section show one-hour ozone concentrations overlaid with the corresponding observations for two periods, one in May and one in September 2012. The plots show

concentrations in the morning, noon, early afternoon, and early evening and follow the development of both observed and modeled ozone through the respective periods.

5.1 May 16 and 17, 2012

Figure 5-1: Modeled and Observed Ozone Concentrations on May 16, 2012 shows four spatial ozone plots for the day. The upper-left panel (06:00) shows very low observed and modeled ozone concentrations across the area depicted, with the lowest in downtown Houston and along the Ship Channel. These low concentrations result from overnight NO_X emissions in the boundary layer titrating any ozone left over from the day before. The upper-right panel shows that by noon a large plume of moderate ozone had formed and was drifting southwestward. The model agrees well with the observations during this period, and also at 14:00 (lower-left panel) and at 17:00 (lower-right panel) as the plume advected to the west.

May 17 showed near-zero modeled ozone concentrations in the area near the Ship Channel at 04:00, as shown in the upper-left panel of Figure 5-2: *Modeled and Observed Ozone Concentrations on May 17, 2012*. Observed concentrations were only slightly higher. By 10:00 (upper-left panel) both the model and monitors showed a large area of moderate ozone to the south and west of the city. By 12:00 the stagnant conditions had built up concentrations over 100 ppb, although the highest observed concentration at Manvel Croix Park - C84 is several kilometers southeast from the modeled peak in West Houston. Simultaneously, the model developed a large pool of ozone over the Gulf. Finally, at 14:00 the model peaked at 96 ppb at Northwest Harris County - C26, matching the observed concentration of 93 ppb (lower right panel). The model missed the observed peak of 103 ppb at West Houston - C554 since the model had its highest concentrations a few kilometers north, but overall the model did a credible job of replicating observed ozone temporally, spatially, and in magnitude over this two-day period.

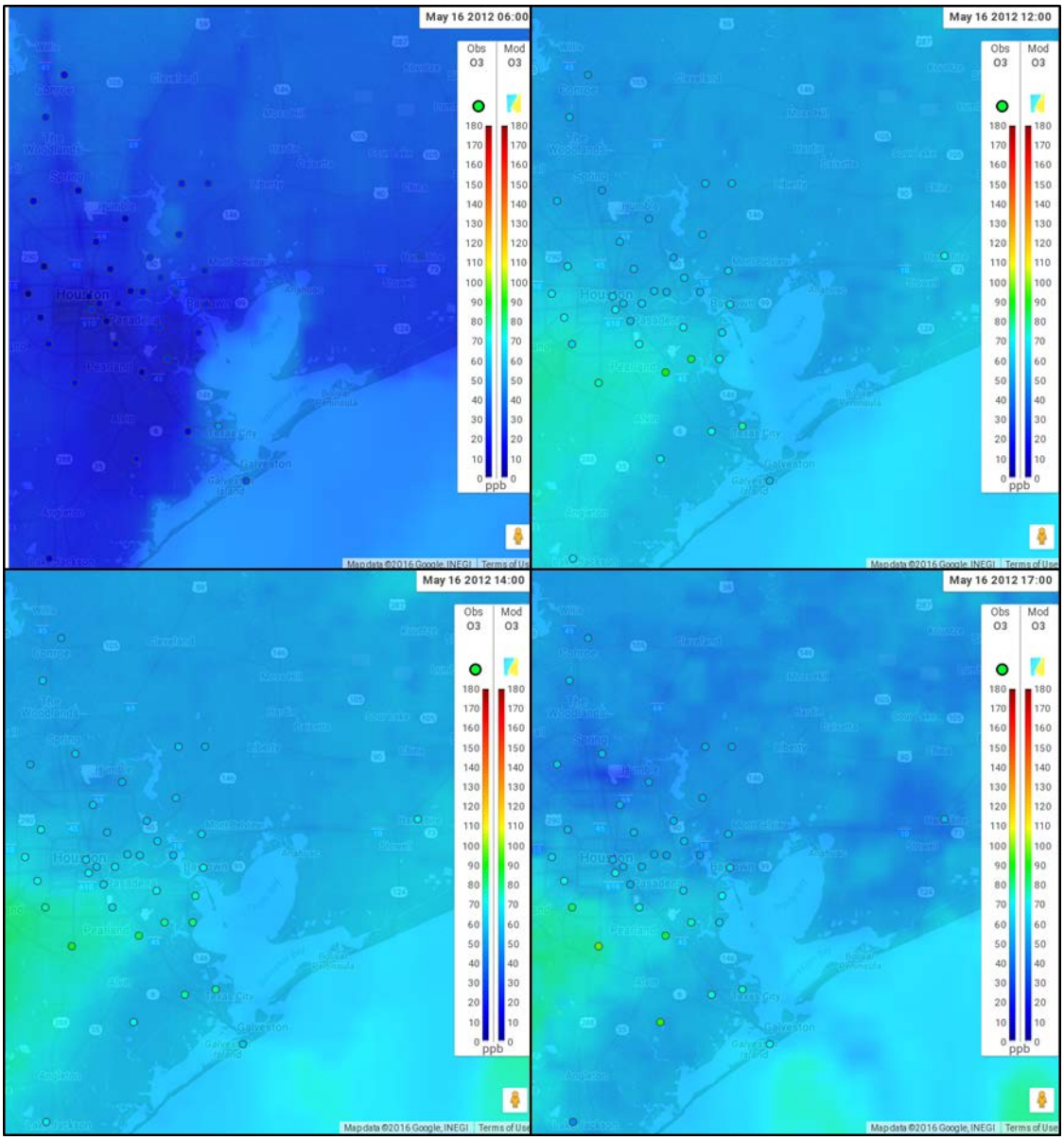

Figure 5-1: Modeled and Observed Ozone Concentrations on May 16, 2012

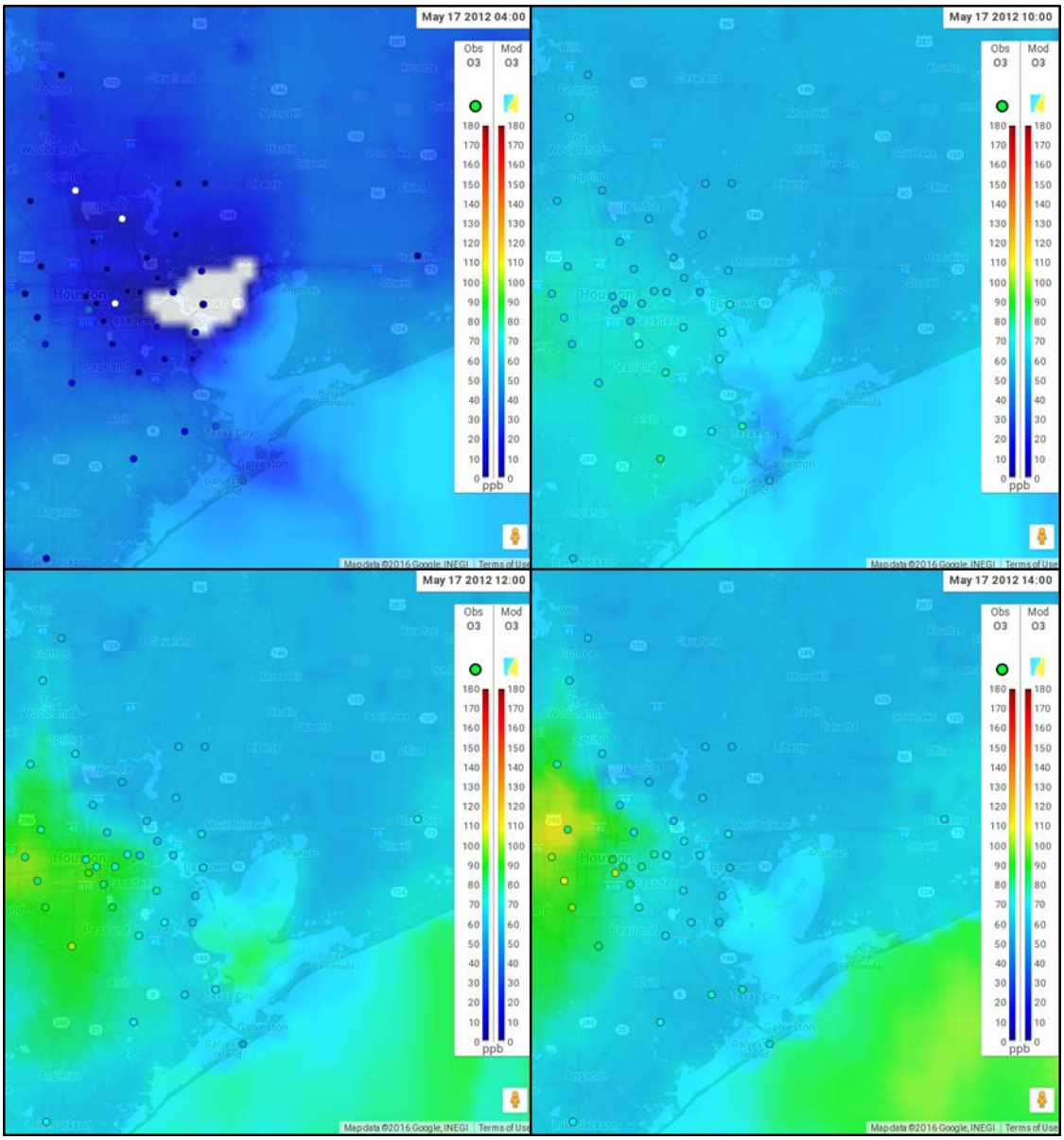

Figure 5-2: Modeled and Observed Ozone Concentrations on May 17, 2012

5.2 September 19 through 21, 2012

September 19 through 21 was similar to the May period shown above. Figure 5-3: *Modeled and Observed Ozone Concentrations on September 19, 2012* shows very low observed and modeled ozone at 06:00 on September 19 (upper left panel). By 12:00 the model accurately places its highest ozone concentrations south and west of downtown Houston (upper right panel). The model captures well the slow southwest drift of the highest concentrations at 14:00 (lower left panel), but under-predicted the 85 ppb concentration at Manvel Croix Park - C84 by 21 ppb. The model peak is several kilometers southwest of Manvel Croix Park – C84 and was lower than observed peaks on that day, most likely due to modeled winds that were stronger and more organized than observed. Figure 5-4: *Section of Map Showing Observed and Modeled Wind Vectors at 14:00 on September 19, 2012* shows a portion of the wind map at 14:00 – modeled winds are shown in blue while observations are shown in red. The upper right panel of the ozone

concentration plot shows that by 18:00 the ozone plume was far to the southwest and very low ozone concentrations covered most of Houston.

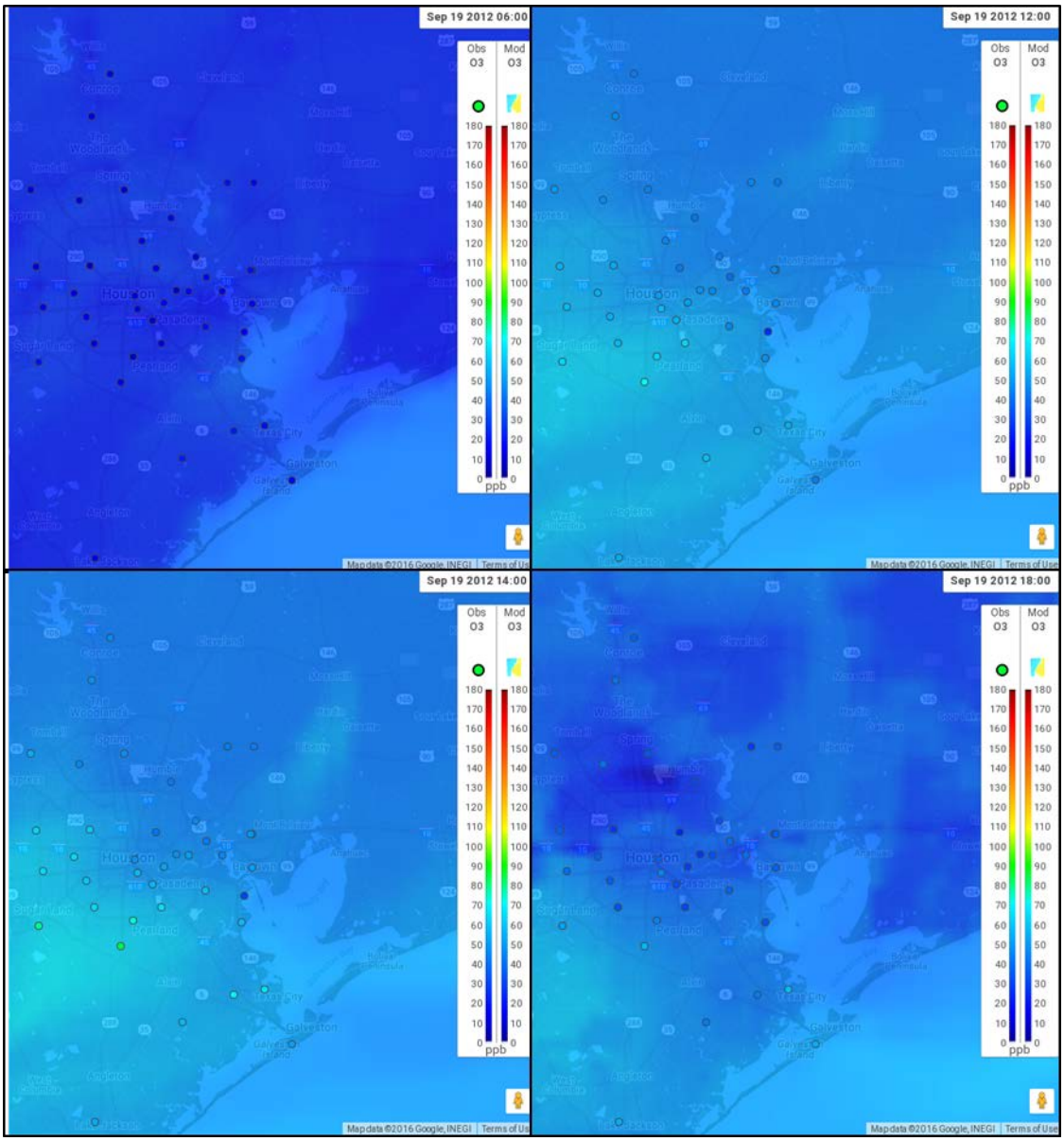

Figure 5-3: Modeled and Observed Ozone Concentrations on September 19, 2012

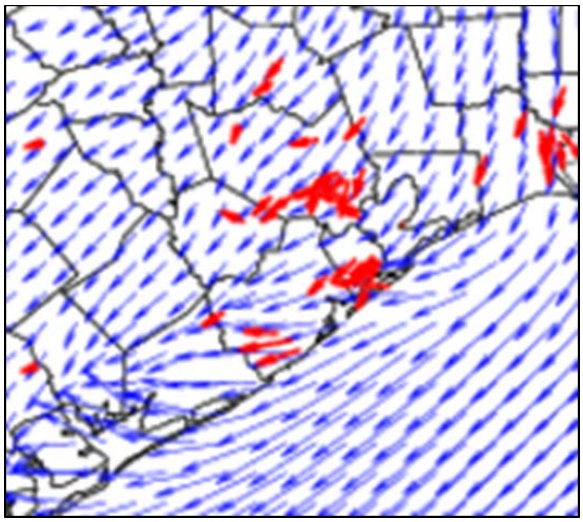

Figure 5-4: Section of Map Showing Observed and Modeled Wind Vectors at 14:00 on September 19, 2012

September 20 was similar to the previous day, except for a more westerly drift. Again too-strong modeled winds were responsible for pushing the ozone plume too far west and not allowing enough time to develop the peak one-hour concentration of 106 ppb observes at Manvel Croix Park – C84 on this day. Figure 5-5: *Modeled and Observed Ozone Concentrations on September 20, 2012* follows the same sequence as the previous figure: upper left o6:00, upper right 12:00, lower left 14:00, lower right 18:00.

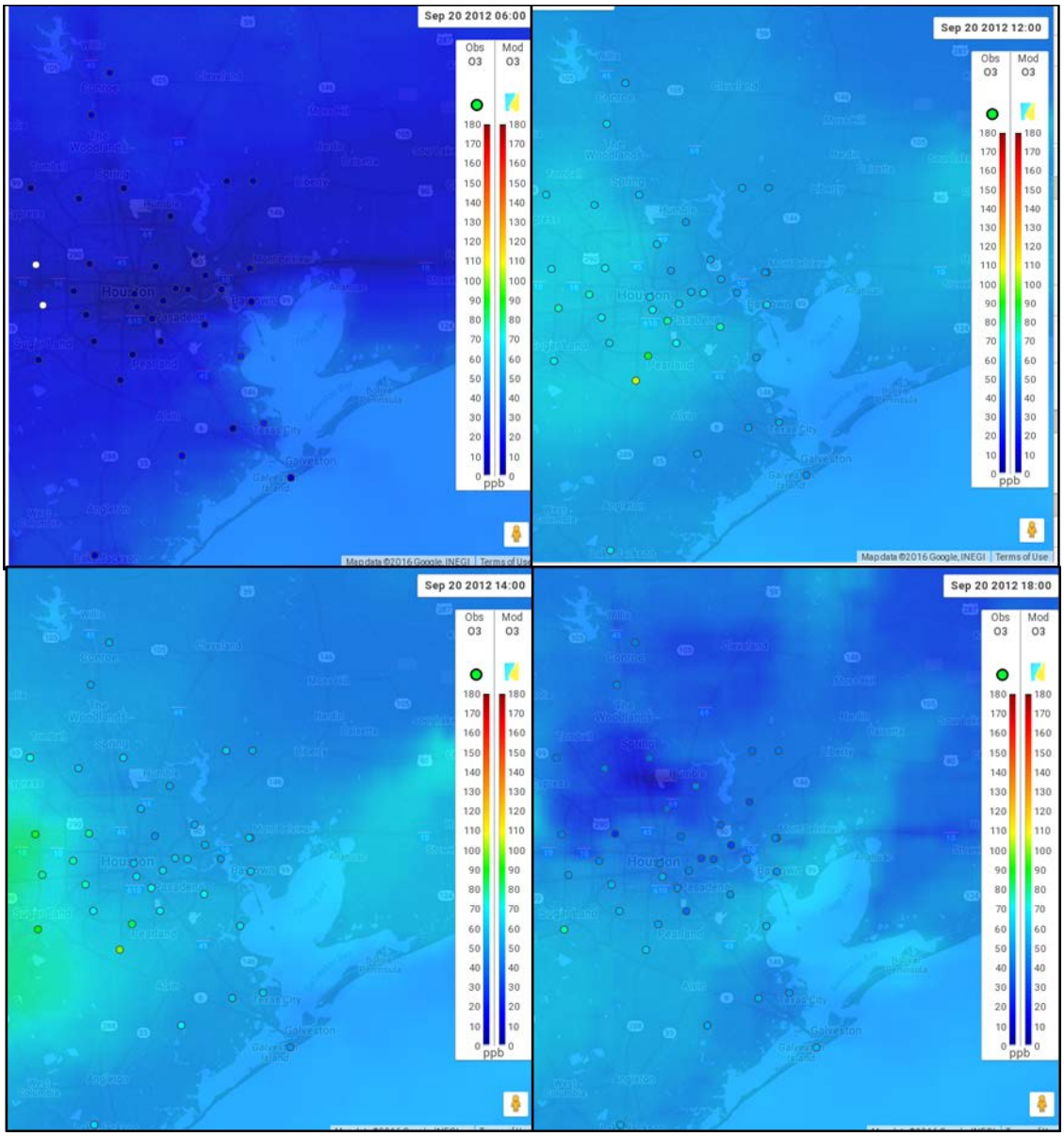

Figure 5-5: Modeled and Observed Ozone Concentrations on September 20, 2012

September 21 provided some relief for Manvel Croix Park by pushing the highest ozone almost due west (*Figure 5-6: Modeled and Observed Ozone Concentrations on September 21, 2012*). Similar to the two preceding days, the model does a very good job of moving the ozone plume in the correct direction. However, the model is unable to match the observed high concentrations at 14:00 seen at West Houston - C554 (106 ppb) or Lang - C408 (108 ppb) because of stronger and more organized winds than observed (Figure 5-7: *Section of Map Showing Observed and Modeled Wind Vectors at 14:00 on September 21, 2012*).

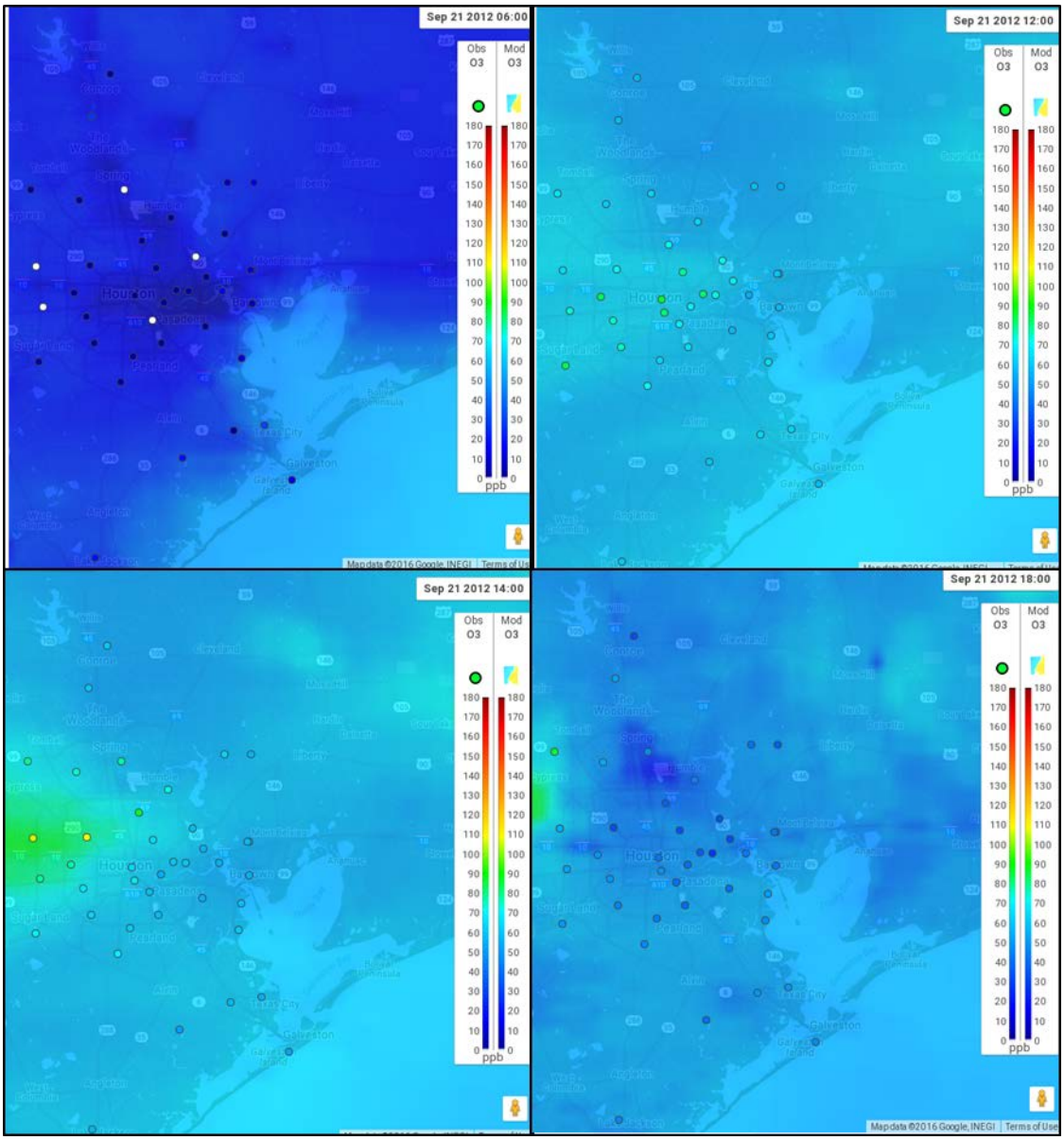

Figure 5-6: Modeled and Observed Ozone Concentrations on September 21, 2012

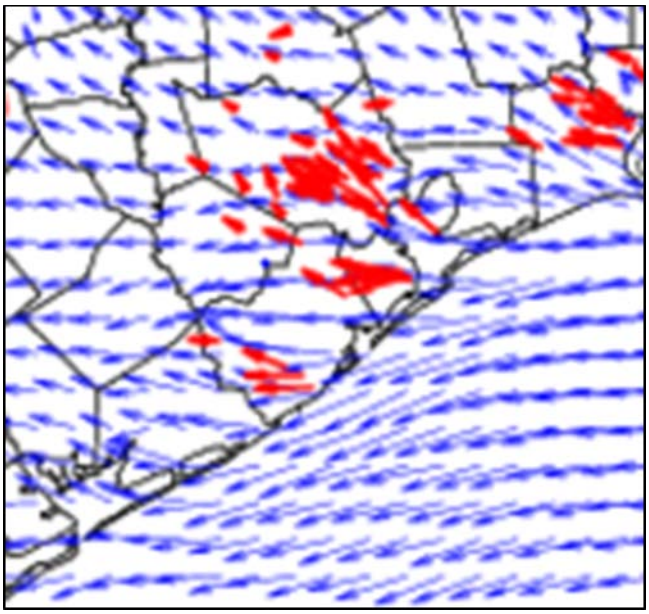

Figure 5-7: Section of Map Showing Observed and Modeled Wind Vectors at 14:00 on September 21, 2012

6. SUMMARY

Two selected episodic periods within the 2012 modeling platform illustrate the model's considerable skill in matching the time and placement of the observed ozone plumes. In the May period, the model matched the observations very well spatially, temporally, and in magnitude. In the September period the model also matched the observed ozone concentrations in time and direction, but higher-than-observed winds tended to push the highest concentrations farther from the city and also diminished the intensity of the ozone concentration peaks. Overall, however, the model is doing a very credible job of replicating ozone production in the region.